

Spintronics

Vishal Ranjan, S1951041

Supervisor: Prof. Bart Van Wees, Group of Nanodevices, Zernike Institute of Advanced Materials, Rijksuniversiteit Groningen, 9747 AG, Groningen, The Netherlands.

Abstract—This review paper describes a new archetype of electronic devices which rely on spin degree of freedom of electrons. These devices have continued to overshadow present charge based devices and show immense promise to overhaul completely in near future for its potential advantages of non volatility, increased data processing speed, decreased electric power consumption, and increased integration densities. However, successful achieving of this requires a complete understanding and optimization of processes such as spin injection, its polarized transport across heterostructure and its spin dependent detection in nanoscale structures. Present review focuses on these challenges elucidating the physics through theory and some important recent experimental works. In addition, historical evolution of the spin based devices and possible conceptualization and fabrication of new devices have also been discussed.

lived up to its expectations. However, Scaling down to really small sizes had limits due to quantum effects. Inclusion of second degree of freedom hence, i.e the spin, in place of or with electronic charge has added a whole new dimensionality to the science and engineering of devices. This idea quickly flourished into what is called spintronics, i.e electronics of spin, (sometimes also called magnetoelectronics) and would hopefully continue to oblige with the Moore's law.

The trigger of spintronics can be correctly attributed to the discovery of Giantmagnetoresistance (GMR) effect in thin films. The name comes from the fact that an assembly of thin films of alternate magnetic and nonmagnetic materials show a huge magnetoresistance. The phenomenon magnetoresistance (MR) is the change of resistance of a conductor when it is placed in an external magnetic field. For ferromagnets like iron, cobalt and nickel this property will also depend on the direction of the external field relative to the direction of the current through the magnet. In general, magnetoresistance effects observed before 1988 were very small, with the highest reported values in the range of a few percent. GMR technology has now translated into unbelievable storage capacity of hard disks and Magnetic Random access memories (MRAM). Hard disk capacity boom is no news now however MRAM are still to conquer commercially.

Apart from the devices mentioned above, there are a number of others in development exploiting the spin degree of freedom. Generally speaking devices of this kind work in the following way. The electronic spin which is double degenerate can be zeeman split in presence of an intrinsic magnetization or external magnetic field. They can be hence polarized in one particular direction using high enough magnetic field in a free magnetic layer 1. This spin polarized electrons are then allowed to carry information (e.g. in form of current) through a nonmagnetic layer 2 and then into another magnetic (a pinned ferromagnet in a particular direction) layer 3. These electrons scatter differently in the interface of layers 2-3 for the different polarization or extent of alignment in the layer 1 and hence form the heart of the active electronics.

Spintronics tops off conventional charge carrier devices with many advantages. One if them is nonvolatility which used that the fact that spin do not require a constant power for sustenance. This also means a low power consumption. Again, spin based devices read electrical resistance between a pair of spin regions. This hence helps in effecting high speed of reading/writing and also high density of device units.

One of the imperative requirements in spintronics is to understand and control the spin transport. We need to optimize spin lifetimes and sustain spin polarized currents through a desirable length scale and across hetero interfaces. Equiva-

CONTENTS

I	Introduction	1
II	Present Spin Based Devices	2
II-A	Spin Valve	3
II-B	Magnetic Tunnel Junction	3
II-C	Galvanic Isolator	4
II-D	Magnetic Random Access Memory	4
III	Spin injection and transport	5
III-A	Ohmic injection	5
III-B	Tunnel injection	7
III-C	Ballistic and hot electron injection	9
III-D	Spin transport and detection	11
III-E	Spin torque	13
IV	Future devices and challenges	14
IV-A	Ferromagnetic semiconductor	14
IV-B	Spin Hall effect	15
IV-C	Graphene	16
IV-D	Bychkov-Rashba structure asymmetry	18
IV-E	Spin transistors and qubits	18
V	Conclusion	20
	References	20

I. INTRODUCTION

THE discovery of quantum mechanical spin angular momentum of electrons was bound to inspire scientists across the globe for its exploitation in practical applications. We have already witnessed a myriad of devices based on electronic charge gifted with both compactness and efficiency. Further to its leverage, Moore's prediction on doubling of transistors per square inch on integrated circuits has remarkably

lently, an efficient method of spin injection and spin transport through the materials needs to be developed. Further we need accurate methods to measure spin coherence in fast enough time scales. This puts further pressure on device scientists to study and understand intensely about spin interactions, its transport in the solid state materials which will also involve knowing effects of this dynamics brought about by defects, dimensionality, electronic band structure and external fields. Moreover, application of optics and magnetisms together with spintronics are worthwhile to explore.

Current literature survey is organized as follows. Second section summarizes some of the important spin based devices realized so far. Third section describes some of the conventional methods of spin injection and transport through materials and interfaces. This section together with next, which lists a few major challenges of future spintronics, form the focus of this essay next section. It would also cover some of the concept future devices which have been contemplated very recently. Finally, there is a conclusion summarizing this report with a hint of personal direction suggested to the present research.

II. PRESENT SPIN BASED DEVICES

GMR was independently discovered in Fe/Cr multi thin layers by two scientists. One was headed by Peter Grunberg at the Julich Research Centre. The other was headed by Albert Fert of the University of Paris-Sud. [1,2] Both used an assembly of thin layers such that Cr (Non magnetic) was sandwiched between two layers of Fe (ferromagnetic). In the absence of an applied magnetic field ($H=0$) the direction of magnetization of adjacent ferromagnetic layers is antiparallel (due to a weak anti-ferromagnetic coupling between layers). In this configuration, the resistance (R) of the assembly is high. When the magnetization vectors of adjacent layers align due to an external field (H), the resistance of the assembly decreases. Fig. 1 shows this behavior for different thickness of Cr layer chosen.

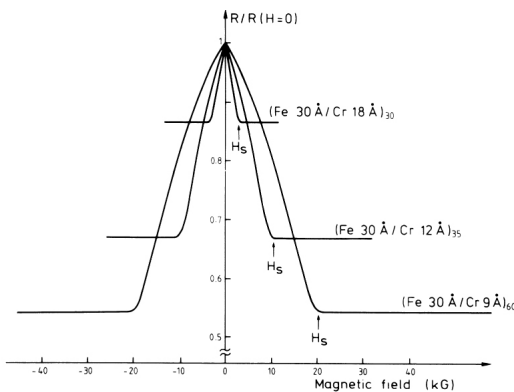


Figure 1. A graph of variation in magnetoresistance of an Fe/Cr/Fe superlattice against magnetic field measured for different thicknesses of Cr layer while keeping thickness of Fe layer constant at 30Å. [1]

Clearly, on decreasing the thickness of Cr layers weak antiferromagnetic coupling between Fe layers strengthens and a better magnetic field was required to saturate the Fe layers

aligned parallel. More importantly, with increasing Cr thickness or temperature, probability of spin flip scattering within Cr layers increases and weakens the magnetoresistance. [1] Note that, the above measurement was taken at 4.2K. Similar effect was also found in Co/Au/Co multilayers by Grunberg. [2]

Why did the two scientists choose above arrangement? Spin polarized currents can be found the materials with imbalance in spin up and down electrons at Fermi level. Ferromagnetic materials serve best example for this case where density of states (DOS) for two states are almost the same however are shifted in energy. Shown in figure 2 are the DOS for spin up and down states in the ferromagnetic and normal metals. Following the spin exclusion at normal and ferromagnetic metal interface, antiparallel alignment suffers a disallowed channel and hence a big resistance. [3]

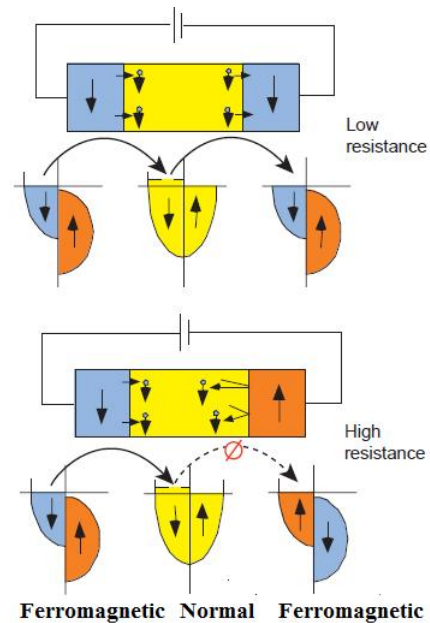


Figure 2. Schematic representations of spin-polarized density of states and transport from a ferromagnetic metal, through a normal metal, and into a second ferromagnetic metal. Top shows a case of low resistance when magnetic moments are parallel, bottom shows the vice versa (ϕ disallowed channel). [3]

A research carried at IBM research division in 1992 showed theoretically an explicit dependence of magnetoresistance ($\Delta R/R$) on thickness of free ferromagnetic layers. [4] (Fig. 3). Since spins have lifetimes, it produce an active layer of ferromagnet responsible for spin polarized currents. At higher thickness, inactive part just adds to the shunting of the current and higher R resulting into a hyperbolic decrease in MR. Its decrease below a characteristic thickness is not fully understood. One reason is obviously absence of outgoing electrons with longer mean free path from the layer.

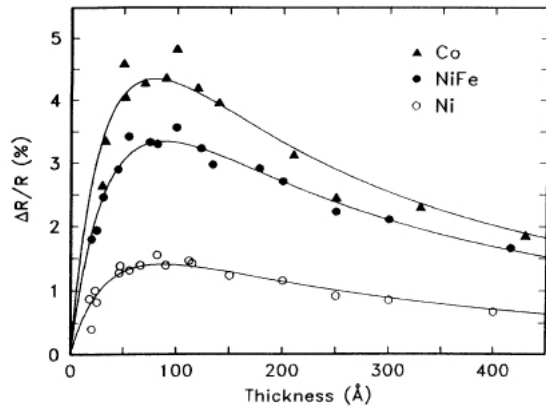


Figure 3. Dependence of Magnetoresistance versus the thickness of free magnetic layer at room temperature. [4]

A. Spin Valve

Spin valve was an immediate consequence of the GMR discovery. The device is shown in the figure 4 and works in a manner as explained in the preceding paragraph (description of spin polarized current through Ferromagnetic-nonmagnetic-Ferromagnetic layers). To get a pinned ferromagnetic layer, an antiferromagnet was juxtaposed with a ferromagnet with a strong magnetic coupling, which hence provided the much needed immunity against any external stray magnetic fields. As magnetization changes from parallel to antiparallel alignment, resistance if the spin valve changes between 5% to 10%. Generally Fe, Ni and Co alloys are used for magnetic layers and Cu for nonmagnetic middle layer. [5] However, there is still hunt for materials with higher MR effect, thermal stability and corrosion resistance.

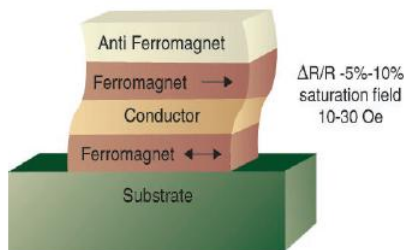


Figure 4. A typical Spin valve; top antiferromagnet is used to pin the magnetization of adjacent layer. Bottom layer is a free ferromagnet layer separated by conductor from the pinned one so that its magnetization can be changed without affecting the former. [5]

B. Magnetic Tunnel Junction

A magnetic tunnel junction (MTJ) is a device in which a pinned layer and a free layer are separated by a very thin insulating layer, commonly aluminum oxide Fig 5. Here the simple pinned layer was replaced with a synthetic antiferromagnet: two magnetic layers separated by a very thin (~10 Å)

nonmagnetic conductor, usually ruthenium. [5] In this way, the strong antiparallel coupling between magnetic layers improves both stand-off magnetic fields and the temperature of operation of the MTJ.

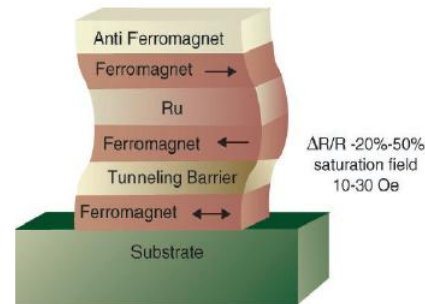


Figure 5. A typical MTJ; similar to spin valve except that pinned layer has been replaced by a synthetic antiferromagnet and separating layer is now an insulator (see text). [5]

Very early in the research on MTJ, Ferromagnetic-Insulator-Ferromagnetic tunneling was shown to have more than 10% magnetoresistance with fields much less than 100Oe at room temperature. An added advantage was the great reproducibility of results. [6] Unlike metal, tunnel barrier offers a very high resistance for both spin up and down electrons and transport occurs through quantum mechanical tunneling. The probability of electrons hence scattering back into first ferromagnetic layer is low and facilitates spin polarized current injection more efficient than metallic systems. As expected tunneling magnetoresistance (TMR) increases with decreasing temperature and can go to as high as 50%. Further, with increasing DC bias this change drops because of enhanced scattering events owing to higher energy.

A work carried by Miyazaki et al showed the dependence of the potential barrier versus tunneling barrier width and then magnetoresistance versus potential barrier for different junctions. [7] It was found that potential barrier height decreases as the square of the inverse of barrier width. Since tunneling current also decays with greater width and height, final magnetoresistance curve versus barrier height should not be monotonic. Indeed it was observed that tunneling magnetoresistance becomes really low for certain range of barrier height and rises again on either side (A kind of local minima). MTJ showed its potential to be used in memory or sensor devices for following reasons. The device operation does not depend much on the thickness of the ferromagnetic layers and insulator layer and with a size of submicron, the device still has reasonable tunnel resistance and favors possible use with low power dissipation. [6]

Invention of spin valve and MTJ have greatly influenced the hard disk density. The conventional read heads used electromagnetic induction to sense the magnetic states of the memory domains. Since the area of the induction capture to have enough power and to prevent false reading was too big, Hard disks could not achieve that density boom.

C. Galvanic Isolator

Galvanic isolation is a principle where two circuits can convey information without transferring charge across them. This is quite important in electrical communications where two circuits may have grounds at different potentials and a cable connection between them can create a ground loop and cause signal degradation. Primitive technology to achieve this was to introduce optical isolators. However this lacked speed and a limit on the frequency transmitted (10MHz). GMR based galvanic isolators are 10 to 100 times faster than optical ones (more than 200 MHz). Further it can withstand 4000V dc of galvanic isolation and requires less than even 1mm² per isolator channel. [8] An analogy between an optical and galvanic isolator has been represented in figure 6.

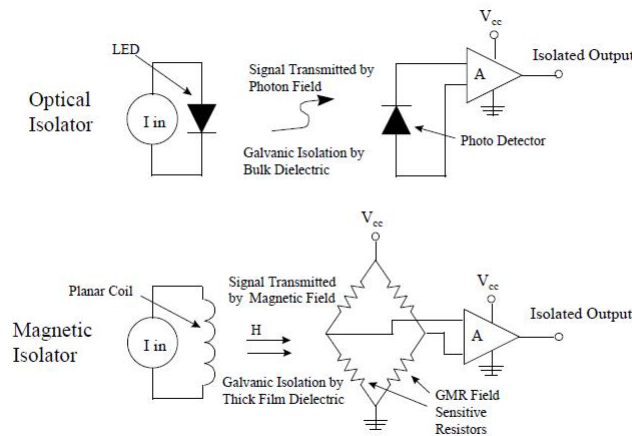


Figure 6. Analogy between GMR isolator and conventional opto-isolator (see text). [8]

A magnetic field proportional to input current signal is generated beneath the coil winding which in turn is sensed across a thick polymer dielectric film by a GMR resistor structure. The dielectric barrier provides high voltage hold-off capability. The sensed magnetic field changes the resistance of the GMR structure proportional to its magnitude. Together with other integrated electronics this change can be quantified to give a desired output proportional to input. Speed of this device can be too high because the GMR material can be switched in less than one nanosecond. The bottleneck in frequency performance results only from the associated silicon electronics. Note that a conventional isolator uses an LED to transform current to electricity and then a photodiode to change back to output current.

D. Magnetic Random Access Memory

The greatest impact of spin-electronic devices is expected to be in magnetic random access memories (MRAM). These can then be used with, or as replacements for EEPROM (electrically erasable, programmable read-only memory) and flash memory in computer applications, where MRAM's lower writing energy, faster writing times, and no wear-out with writing cycle become significant factors. An Added advantage

of this type of RAM is that the data is retained even after power off unlike conventional RAMs used now a days. Although prototype MRAM devices have been employed in some applications, commercial quantities of MRAM are not yet available. Generally speaking MRAM used magnetic hysteresis to write and store and magnetoresistance to read data. Two major memory cells prototypes have been built and are based on GMR based MTJ and Pseudo spin valve. They are described in detail in the following paragraphs.

A simplified GMR based MRAM memory cell looks like as shown in the figure 7. Each cell is surrounded by two wires at right angles to each other (one above and one below the cell, only one shown here). When we desire to write to a cell, we pass current through the required wires. The sum of currents from both wires is used to program a bit. Thus, a magnetic field is induced at the junction. The free plate will pick up this magnetic field, and will get biased in the desired direction. This method is gradually became obsolete due to the fact that high currents are needed in order to write to the cells, and this can lead to prohibitively high power costs.

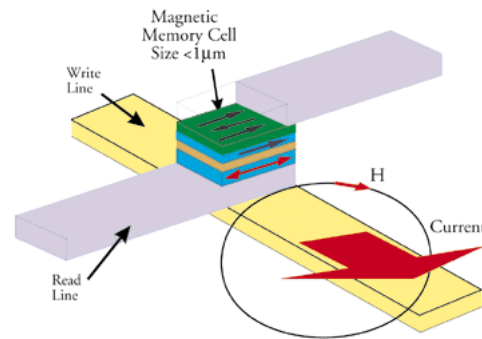


Figure 7. A memory cell of MTJ based MRAM. [taken from Internet]

Katti et al [9] proposed an unconventional spin valve naming it pseudo spin valve. Here, none of the magnetic layers are pinned but are uni-axially free to align. In other words, coercivities of two ferromagnetic layers are chosen in such a way that one acts as a soft magnet while the other hard magnet along a common axis. The middle layer, i.e. nonmagnetic layer, is needed again to facilitate free toggle of magnetization in one layer without affecting the other one. Absence of pinning also makes it imperative to have a thicker middle layer to eliminate any magnetic interaction. In absence of any magnetic field, two layers align along their easy axis which can be chosen one bit of the binary information. Upon application of magnetic field, magnetization of only one layer changes while keeping the parent magnetization of the other one. This state can now be used as the second bit of the binary.

The next generation method of writing to an MRAM cell employs the Spin Transfer Switching mechanism. This is a fairly advanced and recent method. It is based on changing the spin of storage electrons directly with an electrical current rather than an induced magnetic field. This lowers the amount of current needed to write the cells, making it about the same as the read process. (Details of spin transfer switching also called spin torque will be presented in the next section). Fur-

ther methods and designs of MRAM investigated are Magneto thermal MRAM and vertical transport MRAM. M-T MRAM uses a combination of magnetic fields and ultra-fast heating from electrical current pulses to reduce the energy required to write data. Vertical Transport MRAM (VMRAM) is a high-density type of MRAM that employs current perpendicular to the plane to switch spintronic memory elements. [10]

Why MRAMs have failed to capture market so far? One of them is high power requirement for writing which is at least 5 times bigger than read power. High Read out speed also demands high power. Further, there is a limit on how much we can scale down. As we reach a certain critical cell size, the induced field might be picked up by adjoining free plates as well, thus leading to a situation when we write a wrong bit to an adjacent cell. This is called half select problem. So unless spin transfer techniques are optimized the density of MRAM will be lesser than that of conventional DRAMs. Other problems include thermal flip of the layers and the same against stray magnetic fields. Despite these challenges, MRAM research shows a promising stand on low power consumption and high speed memory units. In further years to come, this hence will truly emerge as the universal memory unit of our devices.

III. SPIN INJECTION AND TRANSPORT

Effective operation of spintronics depends on effective spin injection and transport. In any device there are always hetero-metal interfaces. Further, We also need to hook up spin systems with semiconductors to achieve novel better devices. Since the mean free path of electrons differ in different materials, it is imperative to study the nature and effect of the interfaces on the spin polarized current. For practical applications, it is also important that the generation, injection, and detection of such spin currents be accomplished without requiring the use of extremely strong magnetic fields and that these processes be effective at or above room temperature. The use of ferromagnetic metallic electrodes hence appears to be essential for most practical all-electrical spin based devices until and unless useful Ferromagnetic Semiconductors are developed. [5]

In 3d metals, the itinerant electrons are not localized but arranged in bands. The magnetic order in these materials was discussed by Stoner criterion, i.e. the product of the density of states at the Fermi energy and the exchange interaction is larger than a critical value. If the criterion is fulfilled, a splitting of the bands for spin up and spin down electrons occurs and due to the fact that the Fermi energy for both spin directions has to be the same a difference in the occupation for spin up and spin down electrons is caused. Such a situation is present in the 3d ferromagnetic metals Fe, Co and Ni and yields a greater number of so-called majority electrons than of minority electrons resulting in a net magnetic moment. Fig. 8 shows the spin-polarized density of states of Fe which arises by integrating over all states having different wave vectors but the same energy. The exchange splitting between the bands is indicated by the energy E_X .

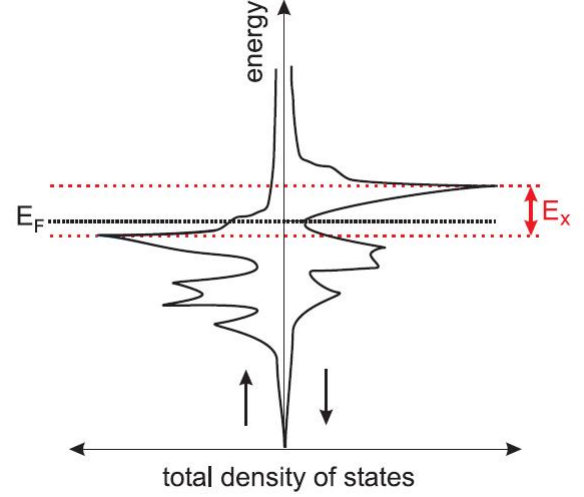


Figure 8. Total density of states of bulk Co showing the exchange splitting by the amount E_X between majority electrons (\uparrow) and minority electrons (\downarrow). The Fermi energy is indicated by E_F . [Taken from Internet]

Another important effect of the exchange splitting is that the Fermi velocities become different for the two spin sub-bands. Further, the scattering potentials for two sub-bands will be different. The direct consequence of these differences is different bulk conductivities for bulk spin up and down electrons.

$$\sigma_{\uparrow,\downarrow} = e^2 N_{\uparrow,\downarrow} D_{\uparrow,\downarrow} \quad (1)$$

where spin dependent diffusion constant given by $D_{\uparrow,\downarrow}$

$$D_{\uparrow,\downarrow} = \frac{1}{3} (v_{F,\uparrow,\downarrow} l_{\uparrow,\downarrow}) \quad (2)$$

Here $\sigma_{\uparrow,\downarrow}$ denotes the spin-up and spin-down conductivity, e is the electronic charge, $N_{\uparrow,\downarrow}$ is the spin dependent DOS at the Fermi energy, $v_{F,\uparrow,\downarrow}$ the average spin dependent Fermi velocity and $l_{\uparrow,\downarrow}$ the average spin dependent electron mean free path. [11] The bulk current polarization can also be defined now.

$$\alpha_F = \frac{\sigma_{\uparrow} - \sigma_{\downarrow}}{\sigma_{\uparrow} + \sigma_{\downarrow}} \quad (3)$$

This parameter will best quantify the quality of the spin conduction and suitability of a material for spintronics. However, Understanding of the sign and magnitude of this parameter is not trivial. This will be explored more in further subsections to come.

A. Ohmic injection

This is the most straight forward method of spin injection. To get ohmic contact between a Ferromagnet and semiconductor, the latter has to be heavily doped allowing a tunnel barrier. Heavy doping however ramps up scattering and spin

flip events eventually decreasing the spin polarized current. Figure 9 shows a ferromagnetic strip connected to a non magnetic metal such that the current flows perpendicular to the interface. Owing to the different conductivities of spin up and down electrons, there is a spin current ($I_{\uparrow} - I_{\downarrow}$) flowing either parallel or antiparallel to the direction of normal charge current ($I_{\uparrow} + I_{\downarrow}$).

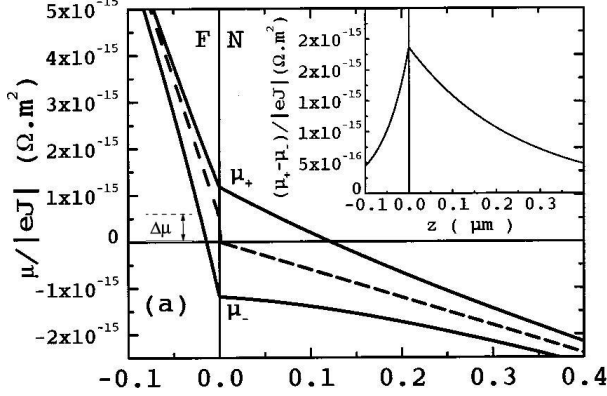


Figure 9. Variation of the electrochemical potentials μ_+ (μ_{\uparrow}) and μ_- (μ_{\downarrow}) as a function of z at a Co/Cu interface. The dashed lines represent the asymptotes. The inset shows the variation of the spin accumulation parameter, $(\mu_{\uparrow} - \mu_{\downarrow})$, as a function of z . [12]

As the electrons move into normal metal, conductivities become spin independent. Following continuities of electrochemical potentials and currents of spin up and down electrons, μ_{\uparrow} and μ_{\downarrow} at the interface split. This phenomenon is called spin accumulation and can be theoretically quantified by $\Delta\mu$ shown in fig 9. Further, the spin polarized current in the bulk ferromagnet converts into a nonpolarised current far away from the interface in the normal metal. Dashed lines represent the extrapolation of the spin electrochemical potentials if there were no spin accumulation on either side and clearly show that it is not continuous at the interface. Hence, theoretically a voltage probe within a distance of spin relaxation lengths could measure $\Delta\mu$ at the interface to quantify spin accumulation. however, the actual noise in the system is comparable and overshadows this measurement. Continuing with the diffusive current flow in ferromagnet, two current densities $J_{\uparrow,\downarrow}$ can be written as as

$$J_{\uparrow,\downarrow} = \frac{\sigma_{\uparrow,\downarrow}}{e} \frac{\partial \mu_{\uparrow,\downarrow}}{\partial x} \quad (4)$$

Assuming that spin flip times for up to go down and vice versa are $\tau_{\uparrow\downarrow}$ and $\tau_{\downarrow\uparrow}$. Continuity of particle requires

$$\frac{1}{e} \nabla_{j_{\uparrow}} = -\frac{n_{\uparrow}}{\tau_{\uparrow\downarrow}} + \frac{n_{\downarrow}}{\tau_{\downarrow\uparrow}} \quad (5)$$

$$\frac{1}{e} \nabla_{j_{\downarrow}} = -\frac{n_{\downarrow}}{\tau_{\downarrow\uparrow}} + \frac{n_{\uparrow}}{\tau_{\uparrow\downarrow}} \quad (6)$$

here n_{\uparrow} and n_{\downarrow} are excess particle density for spin up and down states respectively. Since in equilibrium no net spin scattering occurs, this means

$$\frac{N_{\downarrow}}{\tau_{\downarrow\uparrow}} = \frac{N_{\uparrow}}{\tau_{\uparrow\downarrow}} \quad (7)$$

where N are total DOS for spin up and down states as defined in equation 1. Equations 1 to 7 can be clubbed together to arrive at a simple differential equation 8 governing spin transport in ferromagnet/non magnetic metal. This can be solved using 2 boundary conditions at the interface. First requiring continuity of electrochemical and other that of the spin current densities for both spin up and spin down.

$$D \frac{\partial^2 (\mu_1 - \mu_2)}{\partial x^2} = \frac{(\mu_1 - \mu_2)}{\tau} \quad (8)$$

where $D = D_{\uparrow} D_{\downarrow} (N_{\uparrow} + N_{\downarrow}) / (N_{\uparrow} D_{\uparrow} + N_{\downarrow} D_{\downarrow})$ is the spin averaged diffusion constant, and the spin relaxation time τ is given by $\frac{1}{\tau} = \frac{1}{\tau_{\uparrow\downarrow}} + \frac{1}{\tau_{\downarrow\uparrow}}$. Solving the boundary problem for a ferromagnetic and non magnetic interface fetches the following current polarization. [11]

$$P = \frac{I_{\uparrow} - I_{\downarrow}}{I_{\uparrow} + I_{\downarrow}} = \frac{\alpha_F \sigma_N \lambda_F}{\sigma_N \lambda_F + (1 - \alpha^2 F) \sigma_F \lambda_N} \quad (9)$$

where σ_N and σ_F are conductivities of non magnetic and ferromagnetic regions. λ_F and λ_N are similarly spin relaxation lengths defined as $\lambda = \sqrt{D\tau}$. Note that for non magnets $D_{\uparrow} = D_{\downarrow}$. Also, the spin flip times will be also be the same here. α_F is same as defined in eqn 3. Clearly when non magnetic material is a metal $\sigma_F \leq \sigma_N$ and hence a substantial spin injection could occur. The only limitation here is spin relaxation length λ_F which is generally much smaller than λ_N and hence spin polarized current across metallic interfaces is not efficient. Again, when the N is a semiconductor $\sigma_F \gg \sigma_N$. Consequently the spin injection is extremely low. This problem is called conductivity mismatch and manifests a property of spin injection across the interface strongly dependent on the ratios of conductivity of F and N layers.

Ohmic injection across F/superconductor junction follows a process called Andreev Reflection for energies below the superconducting gap Δ . This means that an electron with spin up enters into superconductor as a cooper pair with spin zero and to conserve the angular momentum and charge, a hole of spin down is reflected back into F. To quantify spin accumulation in this system, equation 8 here then would be solved with new boundary conditions i.e. at $z=0, 1$) $\mu_{\uparrow} = -\mu_{\downarrow}$ 2) $J_{\uparrow} = J_{\downarrow}$. Second condition comes from the fact that total cooper pair spin current in superconductor is zero. This also means that there is a spin accumulation in the ferromagnet over a spin relation length. Jedema et al further showed that spin reversal at the interface [11] leads to a spin contact resistance which in turn is attributed to the excess spin density near the interface. This clearly suggests that the physics of such systems can not be explained by substituting superconductor by a normal conductor with infinite conductivity. In latter case 1) boundary condition will be changed to $\mu_{\uparrow} = \mu_{\downarrow} = 0$ and consequently a zero contact resistance. Since there can not exist a net spin current into superconductor, an efficient spin injection would require a phase transition of the material from superconducting state into normal state.

A simple model to quantify the magnetoresistance of F/N/F spin valve is the simple resistor model as shown in the figure 10. Here it is assumed that currents are linear functions of the voltages applied, i.e. Ohm's law. This could be very well considered for the case when $\lambda_N \gg l$.

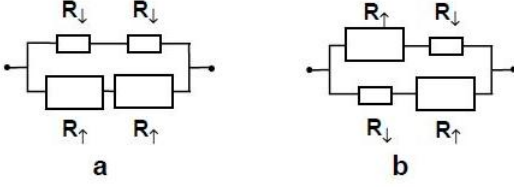


Figure 10. Resistor model for F/N/F spin valve in linear approximation for a) parallel alignment and b) antiparallel alignment. [11]

Here, the resistances R_{\uparrow} and R_{\downarrow} represent the resistances of the spin up and spin down channels. Since the electron has to traverse ferromagnetic and non magnetic metallic distances which are in turn series to each other, these resistances can be written down as the sum of two contributions. The resistance in then non magnetic region will be spin dependent. From resistor model calculations these are found to be [11]

$$R_{\uparrow} = R_{\uparrow}^F + R_{\uparrow}^N = \frac{2\lambda_F}{w(1 + \alpha_F)} R^F + \frac{L}{w} R^N \quad (10)$$

$$R_{\downarrow} = R_{\downarrow}^F + R_{\downarrow}^N = \frac{2\lambda_F}{w(1 - \alpha_F)} R^F + \frac{L}{w} R^N \quad (11)$$

where $R_F = 1/\sigma_F h$ and $R_N = 1/\sigma_N h$ are the square resistances of the ferromagnet and nonmagnetic metal thin films, w and h are the width and height of the nonmagnetic metal strip. Clearly second term is the general resistance of a metallic wire of length L . Two terminal resistances can now be easily calculated. For cases a and b in figure 10, this will be

$$R^{parallel} = \frac{2R_{\downarrow}R_{\uparrow}}{(R_{\downarrow} + R_{\uparrow})} \quad (12)$$

$$R^{antiparallel} = \frac{R_{\downarrow} + R_{\uparrow}}{2} \quad (13)$$

The magnetoresistance hence will be $R^{antiparallel} - R^{parallel}$ given as following,

$$\Delta R = \frac{(R_{\uparrow} - R_{\downarrow})^2}{2(R_{\uparrow} + R_{\downarrow})} \quad (14)$$

The resistances from equation 10 and 11 can be substituted to fetch the following final relation. This relation with proper substitution gets the same form as equation 9.

$$\Delta R = \frac{2\alpha_F^2 \lambda_F^2 R^F}{(1 - \alpha_F^2)^2 L w R^N} \quad (15)$$

Above descriptions to inject spin across semiconductor/metals takes place near or at Fermi level within μV . The method as it seems is quite reasonable in studying physics of the injection however the small voltage and hence small current injection which is comparable to the noise makes it almost unsuitable for practical applications.

B. Tunnel injection

Alvarado and Renaud using a scanning tunneling microscope with a ferromagnetic tip, showed that a vacuum tunneling process can effectively inject spins into a semiconductor. The development of FM-insulator-FM tunnel junctions with high magnetoresistance has also demonstrated that tunnel barriers can result in the conservation of the spin polarization during tunneling, suggesting that tunneling may be a much more effective means for achieving spin injection than diffusive transport. Further, theoretical works carried out by and Fert et al [12] and Rashba and Flatte and co-workers [13] have quantitatively developed the understanding of the potential effectiveness of tunnel injection.

Following the same resistor model, the present case can be represented in a way as shown in figure 11. Top and bottom arms show the resistance carried by spin up and down electrons respectively. To calculate the polarization, we need to find the current in individual arms and apply equation 9. Since two ends have common potential, this would simply fetch us the following equation. $2R_N$ is used because R_N is spin independent Resistance and has been connected in 2 parallel arms.

$$P_{F/I/N} = \frac{(R_{\uparrow}^F + R_{\uparrow}^{TB} + 2R_N) - (R_{\downarrow}^F + R_{\downarrow}^{TB} + 2R_N)}{(R_{\uparrow}^F + R_{\uparrow}^{TB} + 2R_N) + (R_{\downarrow}^F + R_{\downarrow}^{TB} + 2R_N)} \quad (16)$$

where R^{TB} is the spin dependent tunnel barrier resistance and others are defined as per equation 10 and 11. Since $(R_{\uparrow}^{TB} - R_{\downarrow}^{TB}) \gg (R_{\uparrow}^F - R_{\downarrow}^F)$ the above equation simplifies to the following.

$$P_{F/I/N} = \frac{(R_{\uparrow}^{TB} - R_{\downarrow}^{TB})}{(R_{\uparrow}^{TB} + R_{\downarrow}^{TB})} \quad (17)$$

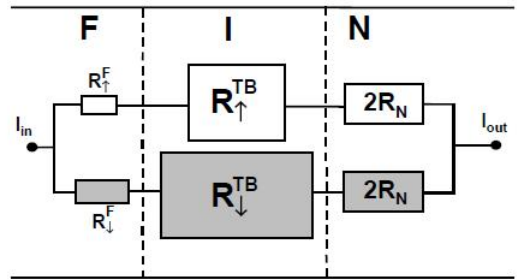


Figure 11. Ferromagnetic-Insulator-Normal metal resistor model. [11]

Tunneling resistance depends on the barrier thickness and potential barrier at interface. Accordingly, if the impedance of a barrier at an interface is sufficiently high, then the transport across that interface will be determined by the density of the electronic states of the two electrodes that are involved in the tunneling process. Note that the density of states will be spin dependent. Since the current through the barrier is then sufficiently so small that the electrodes remain in equilibrium and the relative spin-dependent conductivities of the electrodes play no substantial role in defining

or limiting the spin-dependent transport across the interface. Consequently, negligible or no spin accumulation builds near interface. From last section we saw that for $\sigma_F \gg \sigma_N$ when N is a semiconductor spin injection is severely limited (eqn 9). This is also evident from eqn 16. Substituting $R^{TB} = 0$, means that polarization across the barrier is given by $(R_{\uparrow}^F - R_{\downarrow}^F)/(4R_N + R_{\uparrow}^F + R_{\downarrow}^F)$ which is almost zero if $R_N \gg R^F$, the case for N=semiconductor. However with F-T-N interface the conductivities mismatch are worked away as justified by equation 17. Here polarization is completely dependent on the spin up and spin down barrier tunnel resistances.

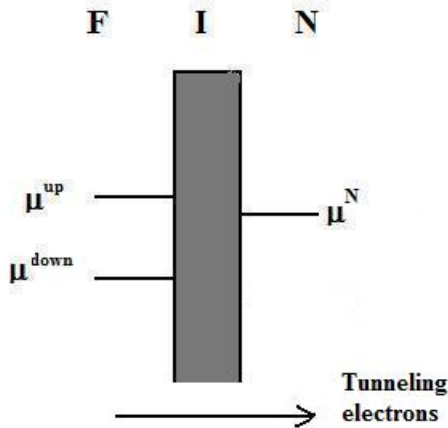


Figure 12. Spin dependent electrochemical potential across and near tunneling interface when resistance of tunneling barrier is much higher than that of F or N. The electrochemical potentials remain in equilibrium with respect to that of normal metal (Fermi energy) and current across the barrier depends on the spin dependent density of states (DOS) of two electrodes. Note that DOS for metal is spin independent.

Electrochemical potential of electrons at an F/I/N interface has been shown in figure 12 along the flow of tunneling electrons. μ^N represents spin independent electrochemical potential of the metal (\sim Fermi energy). Note that far away from the interface in N, owing to spin relaxation, current will be depolarized. In practice a double barrier ferromagnetic tunnel junctions (DFTJ, F/I/F/I/F) have been put a lot in use. First layer is used to ballistically inject electrons into middle layer and the last ferromagnetic layer detects the spin accumulated in the middle layer. (fig 13) These are becoming more and more interesting for their novel spin dependent transport properties such as spin-dependent resonant tunneling [14], spin-dependent single electron tunneling [15], induced magnetization switching and spin accumulation [16]. Unlike in the former metallic systems where spin accumulation is quite small, the magnitude of spin splitting of chemical potential due to spin accumulation in double tunnel junctions can be much larger. These hence serve one of the important systems to investigate spin accumulation. Further, the electrons once injected have minimal probability of scattering back into ferromagnet and hence preserve spin information. Again, the spin relaxation in the material is relatively much stronger than that caused by the voltage probe and it can therefore facilitate an ideal spin voltage probe.

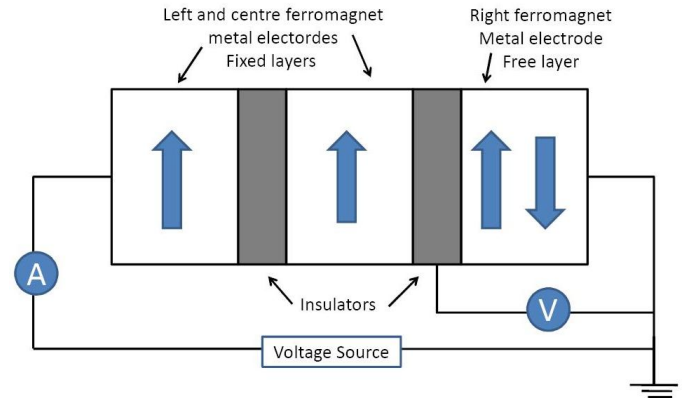


Figure 13. A Double barrier ferromagnetic tunnel junction.

Nozaki et al [14] showed spin dependent tunneling conductance properties in fully epitaxial double MgO barrier magnetic tunnel junction with layered nanoscale Fe layers as middle layer. They showed that conductances as a function of biased voltage were oscillatory. They further showed that the oscillations had a clear connection with the middle layer thickness and magnetization alignment. This effect is amazing understanding that spin dependent quantum well states (quantized energy states) form in the ultra-thin Ferromagnetic middle layer. Further theoretical works in this field have shown that TMR effects enhance at resonant voltages where conductance oscillation reaches a peak value. However, since the reflection of electrons at the interface of metal junctions is imperfect, a double barrier structure is not complete for confinement of electrons and the above mentioned realization of the resonant tunneling effect.

Spin dependent single electron tunneling through a double barrier ferromagnetic tunnel junction was first shown by Bruckl et al [15]. They employed two serial Co/Al₂O₃/Py tunnel junctions with single junction are of 100×200 nm². At low temperatures because of small capacitances device showed both coulomb blockade (0.1 to 2.6 eV) as well as spin dependent tunneling transport. A strong enhancement of coulomb blockade regime in addition to the increasing TMR with decreasing biased voltage was also observed which they explained due to cotunneling effects. (Generally tunnel rate is determined by first order perturbation theory. However in the coulomb blockade regime, where it is very small or even zero at zero kelvin, second order perturbation terms are important. The latter is called cotunneling. In general a circuit with N tunnel junctions will show cotunneling up to Nth order.) However this enhancement method for devices at room temperature is not practical. That would require capacitance as small as aF, which means that the junction area is of order of few nm². This is not accessible from normal lithographic methods.

Electrical detection of spin accumulation in a p-Type GaAs Quantum well was first achieved by Mattana et al [16] using DFTJ. They used a structure GaMnAs/AlAs/GaAs/AlAs/GaMnAs. They observed TMR in this

double junction as large as 38%. This is really interesting because TMR effect is almost negligible for a double tunnel junction in an F/I/N/I/F system. Further, TMR for a single junction is generally double of what it is for double junction if N is a normal metal. Mattana however showed that TMR effect remained same even if one junction was used. They concluded that such effect in semiconductor system must have happened due to a sequential tunneling without spin relaxation in GaAs spacer. This means that the spin relaxation time is much larger than the time spent τ_n by a hole through the thickness. Although they did not observe a similar oscillatory behavior of conductance like Nozaki, they described long relaxation time as a manifestation of quantization of the system. If ϵ_n and T are the quantized energies and transmission coefficients of middle spacer, time spent can be given as

$$\tau_n = \pi\hbar/(\epsilon_n T) \quad (18)$$

The above TMR could not be described by coherent tunneling. This kind of tunneling on quantum states requires that the spatial coherence time of the wave functions in GaAs will be much longer than the mean time spent by a hole. Typical calculations for coherence time together with eqn 18 showed that this condition can not be satisfied.

C. Ballistic and hot electron injection

Ballistic electron injection provides us with an alternate approach for spin injection in ballistic regime (few eV above or below Fermi level also called hot electrons). The probability of spin injection here depends on the difference between the conduction bands of ferromagnetic (spin dependent) and that of semiconductor. Transmission and reflection also assumes that at interfaces transverse momentum of the electrons are conserved.

Tunnel junctions are the ideal hot electron source. The electrostatic potential energy qV provided by voltage bias V tunes the energy of hot electrons emitted from the cathode, and the exponential energy dependence of quantum mechanical tunneling assures a narrow distribution. This is shown in red in figure 14. Metals have a very high density of electrons at and below the Fermi energy E_F . What we want is collection of hot electrons by the semiconductor thus rectifying any contribution from the metal. This is easily achieved by the potential barrier (schottky type) at the interface which is created by the difference in work functions of the metal and the electron affinity of the semiconductor. Since the layers are too thin, in reality its height is determined more by the surface states which lie deep in the bandgap of the semiconductor that pin the Fermi level. [17] Hot electrons thus created can be collected by the Schottky barrier if $qV > q\phi$. There is of course always a leakage current due to thermionic emission over this Schottky barrier at nonzero temperature; because typical barrier heights are in the range 0.6-0.8 eV for the common semiconductors Si and GaAs, hot electron collection with Schottky barriers is often performed at temperatures below ambient conditions to reduce current leakage to negligible levels.

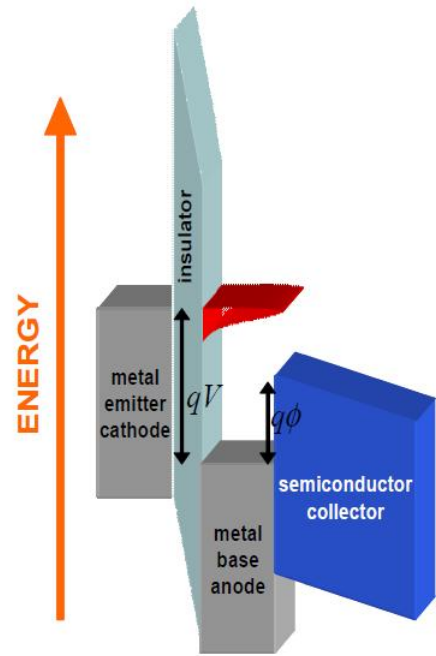


Figure 14. Schematic illustration of a tunnel junction used as a source for ballistic hot electron injection into a semiconductor conduction band. [17]

This transport can be quantified in the following way. Three transport regimes need to be considered. 1. Electrons from the injection tip tunneling into metal 2. transport across the ferromagnet/normal metal 3. injection into semiconductor.

1. First suggested by Bardeen, tunneling from the STM tip into metal can be described by the equation 19 and 20.

$$I = \frac{2\pi e}{\hbar} \sum_{\mu\nu} f(E_\mu)[1 - f(E_\nu + eV)] |M_{\mu\nu}|^2 \delta(E_\mu - E_\nu) \quad (19)$$

$$M_{\mu\nu} = \frac{\hbar^2}{2m} \int dS (\psi_\mu^* \nabla \psi_\nu - \psi_\nu \nabla \psi_\mu^*) \quad (20)$$

here μ and ν represent tip and metal respectively. $f(E)$ is the Fermi function and ψ represent the wave function of the electrons. $M_{\mu\nu}$ represents the tunneling matrix element between the unperturbed electronic states of the tip and metal. The integral in equation 17 is over surface area lying between the vacuum barrier. Due to the fact that electrons tunnel, and assuming no thermal flipping of spins during the process, spin polarization will sustain its character.

2. The electrons will now traverse across the ferromagnetic metal. As shown in the figure 8, majority spin up electrons have lesser density of states above Fermi level compared to that of spin down electrons. This causes two spin types to scatter with different probabilities. The scattering will also in general depend on the energy (velocity), phonons and impurities in the system but these do not discriminate spin up and down. Since there are few states in the excited state for spin up, these will scatter less than the counter part. Representing λ_\uparrow and λ_\downarrow as the attenuation lengths (same as mean free path) of the spin up and down electrons, transmission through the metal shows following exponential decay.

$$T_{\uparrow,\downarrow}(E) = \exp(-d/\lambda_{\uparrow,\downarrow}) \quad (21)$$

After traveling a distance d in the ferromagnet, the initial unpolarized hot electrons will hence be polarized which can be represented as [17]

$$P = \frac{\exp(-\frac{d}{\lambda_{\uparrow}}) - \exp(-\frac{d}{\lambda_{\downarrow}})}{\exp(-\frac{d}{\lambda_{\uparrow}}) + \exp(-\frac{d}{\lambda_{\downarrow}})} \quad (22)$$

3. Polarized electrons then inject across the Schottky type barrier. Again, the conduction sub bands of spin up and down type electrons differ in FM and this further enhances the polarization of the electrons. The transmission probability will be again determined by energy and momentum constraints imposed by the band structure difference between the semiconductor and metal at the interface. The current then will be proportional to

$$I = K \exp\left[\frac{e(V - \phi)}{kT} - 1\right] \quad (23)$$

The injected electrons in semiconductor will have maximum K.E = $E_F + eV - e\phi$. The injection however will be limited spatially. The electrons have different effective masses in the metal and semiconductor. This causes a refraction similar to that of electromagnetic wave at an interface. Consequently, there exists a critical angle after which electrons are internally reflected (outside a cone). This angle will of course depend on the applied voltage and effective mass mismatch. If there occurs no spin flipping at the interface, the ballistic electron current injection can be as high as 90% polarized. Further, the injection energy relative to conduction band of semiconductor can be controlled. [5]

Spin dependent hot electron transport using STM and Ballistic electron magnetic microscopy (BEEM) was first shown by Rippard and Buhrman. [18] They observed the relative magnetic orientation of thin films trilayer Co/Cu/Co during the measurement and could also monitor its change by applying an external magnetic field (which changed the ferromagnetic alignment of Co into antiferromagnetic). From hot electron transmission measurement (1-2V) as a function of Co thickness and relative magnetic alignment, spin attenuation lengths and relative transmission factors, depending on energy, of spin up and down electrons were obtained to a good precision. It was also seen that for very thin (a few Å) Co layers, weakly majority-spin polarized electron beam above 1.3 eV and a minority-spin polarized beam below 1.2 eV. For thicker Co layers the transmitted beam was always majority-spin polarized. Figure 15 shows band diagram of BEEM operating in normal mode. A STM tip is used to inject hot electrons. The middle trilayer acts similar to a spin valve. The tunnel injected unpolarized current is spin filtered by the first ferromagnetic layer and depending on the relative orientation of spins in next magnetic layer, current collected by the semiconductor is low or high.

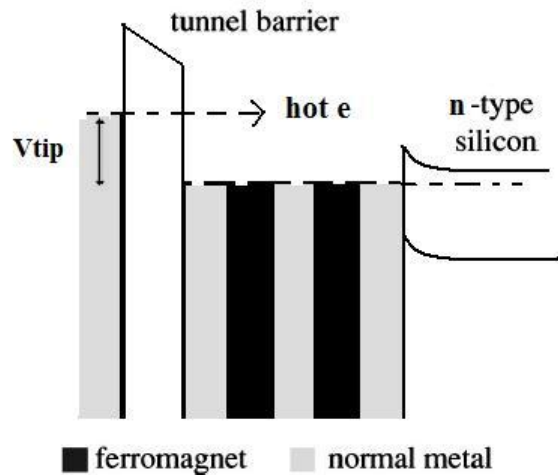


Figure 15. Hot electron transport in BEEM in normal mode. Alternate layers of ferromagnet and normal metal form spin valve which can be tuned in presence of an external magnetic field.

On a similar note, Ballistic hole magnetic microscopy (BHMM) was first successfully shown by Banerjee et al. [19] Here, they used a positive bias of the tip such that a current of hot holes were injected through tunneling (Figure 16b). For Co, they measured the attenuation length increasing from 6 to 10Å with energy range 0.8 to 2 Volts. They also measured change in hole current in a thinfilm trilayer $Ni_{81}Fe_{19}/Au/Co$ as a function of relative alignment of magnetic layers which saw a change by factor of 2.3 for parallel versus antiparallel. Looking back at figure 8, minority spin electrons have large number of empty (excited) states to which hot electrons can decay compared to majority electrons which have few. This reason is sufficient to explain spin filtering of hot electrons. However hot holes have no appreciable difference in the DOS below E_F to which these can decay. Spin filtering of holes (spin asymmetry) as confirmed by Banerjee et al is hence surprising. Transmitted current of holes in normal BHMM was rather low. Banerjee et al then performed first measurements of BHMM in reverse mode. [20] Here the carriers injected from the tip are hot electrons. These decay inelastically in metal and ferromagnet to form electron hole (e-h) pair. Since the hot holes decay length in normal metals are much larger compared to that in ferromagnets, the e-h generation in metal does not affect the analysis of current collected by semiconductor. This mode has been shown schematically in figure 16a.

The reason for spin dependent scattering of holes was then proposed by Banerjee [19]. The attenuation length associated with carriers is not an independent quantity but is a product of inelastic lifetime and group velocity (v_g) of the corresponding spin bands.

$$\lambda_{\uparrow,\downarrow} = \tau_{\uparrow,\downarrow} v_{g\uparrow,\downarrow} \quad (24)$$

In ferromagnet Co, the s and p character of orbitals are reduced due to its hybridization with d orbital. The resultant band has a dip each for minority and majority spin carriers exactly at the place where there was a maxima in d band. Since this dip occurs for majority spin under the Fermi

energy. Consequently, these have smaller group velocity than minority spins resulting in them spending more time in the ferromagnetic layer and being more susceptible to inelastic scattering.

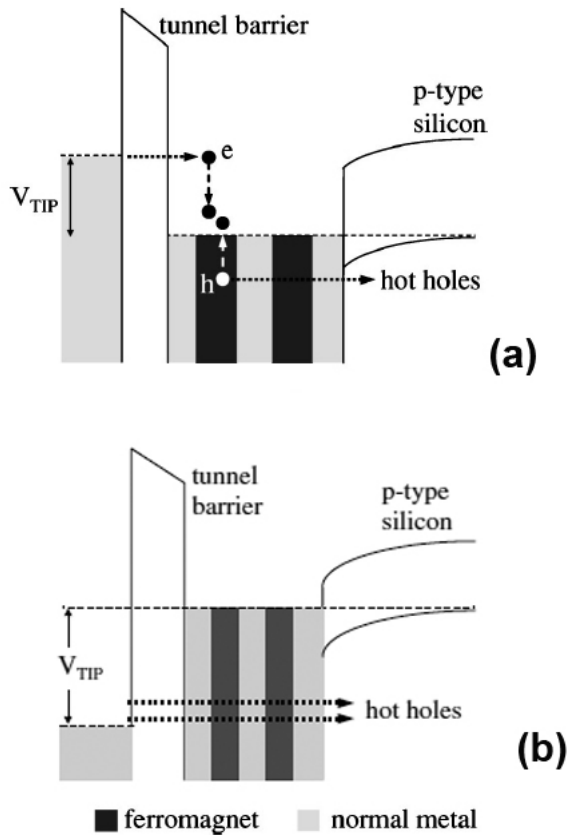


Figure 16. BHMM in (a) reverse mode (b)normal mode. [15,16]

BEEM together with BHMM have been used to image structural and electronic properties with nanoscale resolution using STM tips. Although much of physics behind scattering of polarized hot electrons is only partially understood, its promise in practical uses is immense. One can even achieve a higher resolution than present limits and also get a better understanding of magnetic structures and interfaces and its variation against applied external field.

D. Spin transport and detection

Some of the primary concerns in spintronics are spin life times and coherent spin transport in heterostructure and semiconductors. Further, there are spin flipping scattering at Schottky interface in addition to spin relaxation and spin orbit scattering of hot electrons when passing through the depletion region of semiconductor. It hence becomes highly imperative to understand the spin transport using a scanning probe or nanofabricated device which together with theoretical description can quantify its various aspects. The spin injected electrons in metals and semiconductors are at non equilibrium

and they come to equilibrium via relaxation which is best characterized by relaxation time τ and relaxation length λ .

Also important is spin coherence (spin precession). Treating spin like a classical particle, spin angular momentum under perpendicular magnetic force causes it to precess (Larmor precession) with a Larmor frequency $\omega_L = -g\mu_B B_\perp/\hbar$. Such precession can also result from spin orbit coupling present in the system. Although, a ballistically injected spins would then have a definite evolution profile of spatial and temporal coherence, diffusive case renders it total random.

1. Ballistic case of spin precession: Shown in fig 17 (top) is the evolution of spin precession across a spin valve structure. As electrons move from F1 to F2, they precess and change spin direction depending on the Larmor frequency, i.e. $\phi = \omega_L t$. However, In ballistic case it can be assumed that the time of flight (t) of spins from electrode F1 to F2 is single valued. Since the F2 electrode measures the voltage signal depending on the projection of direction of spins entering it with respect to its magnetization axis, observed signal as a function of precession angle (hence time of flight) will be a perfect cosine as shown in fig 17 (bottom). Clearly increasing the magnetic field would increase the frequency and therefore the roundtrips of spin across the nonmagnetic material N.

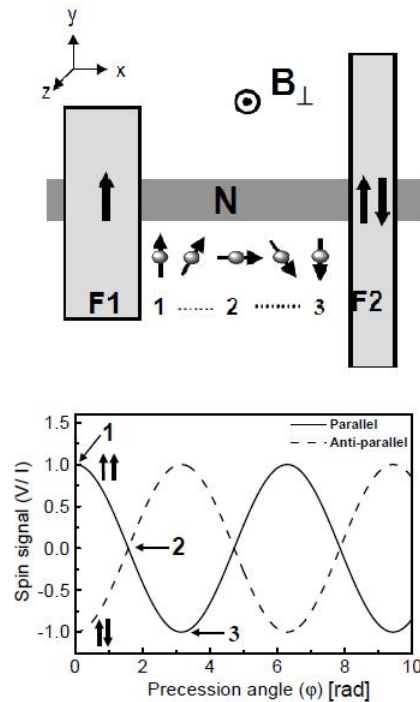


Figure 17. Spin valve signal oscillations due to applied magnetic field. The label 1,2 and 3 refer to a precession angle of 0, 90 and 180 degrees. [11]

2. Diffusive case of spin precession: In this case the travel time between the detector and injector can not be considered unique. This means that spins detected at a distance L from injection point will not have an unique precession angle but must have a distribution owing to different diffusion times

(t)/lengths traveled. The probability of spins with different diffusion times at a distance L can be then quantified by following equation.

$$\varphi(t) = \sqrt{1/4\pi Dt}.exp(-L^2/4Dt).exp(-t/\tau_{sf}) \quad (25)$$

where first exponent describes the normal probability distribution for 1D diffusive conductor while the second exponent takes into account the fact that a spin after an average time τ_{sf} could flip due to spin relaxation. This has been shown in fig 18. Here τ_D represents the peak position ($\partial\varphi(t)/\partial t = 0$). Output signal V/I would be then a summation over all spins with different diffusion times (and precession angle) and hence damped.

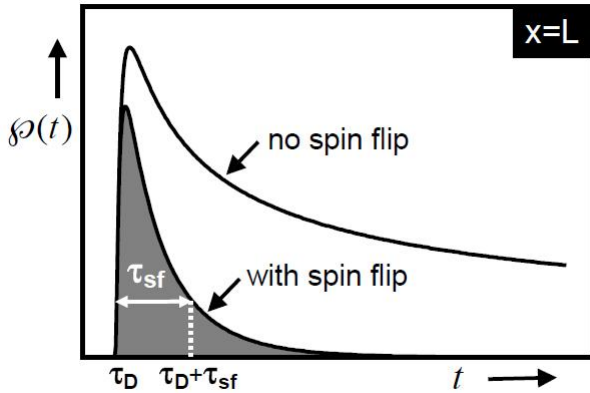


Figure 18. Probability in 1D transport that once an electron is injected will be present at $x=L$ as a function of diffusion time. Unshaded curve shows the case if spin flipping time τ_{sf} is infinite. [11]

Many methods have been proposed to explain spin relaxations in metals and semiconductors some of which follow. Following mechanisms are not exclusive of each other and can coexist.

- 1) *Elliot-Yafet Mechanism*: According to this, A periodic lattice ion induced spin-orbit interaction is modified by phonons and can directly couple the (Pauli) spin-up and spin-down states. This can then couple with momentum scattering caused by impurities and phonons and cause spin relaxation. This effect is quite dominant in small gap semiconductors with large spin orbit coupling. A quantitative quantum mechanical description has accordingly been developed to describe wavefunctions and related relaxation time. [21]
- 2) *D'yakonove-Perel Mechanism*: This mechanism explains the relaxation in systems with no inversion symmetry. Owing to spin orbit interaction and lack of this symmetry electrons start feeling an effective magnetic field. However this magnetic field does not stay constant in all directions and also fluctuate with time. This in turn randomly change the direction and phase of spin precession. Further momentum scattering ensures a momentum dependent spin precession which altogether dephases a spin effectively and causing relaxation. The

effect clearly becomes strong at high temperature and increase in bandgap[21].

- 3) *Bir-Aronov-Pikus Mechanism*: First shown by Bir et al [21] spin relaxation of conduction electrons in p doped semiconductor can happen owing to scattering and its exchange interaction with holes. This exchange is governed by $H = A\vec{S}\cdot\vec{J}\delta(r)$ where where A is proportional to the exchange integral between the conduction and valence states, J is the angular momentum operator for holes, S is the electron-spin operator, and r is the relative position of electrons and holes. Further, the scattering depends on the state of holes which could be degenerate or non degenerate, bound or free on acceptors, fast or slow. This mechanism becomes effective at low temperatures. [21]
- 4) *Hyperfine interaction mechanism*: A hyperfine interaction in material means a magnetic interaction with magnetic moments of nuclei and electrons. Although this is quite weak to cause effective spin relaxation of free electrons in metals or bulk semiconductors as it generally affects the bound electrons, it proves as an important mechanism for ensemble spin dephasing and single spin decoherence of localized electrons confined in quantum dots or bound on donors. [21]

Apart from theoretical understanding of coherence and spin relaxation processes, spin detection techniques are equally important to quantify and verify these parameters for different materials and heterostructures of interest. A typical spin detection would sense the changes in the signal due to spin injection. The non equilibrium spin injection can then result in a voltage or a resistance change which can be measured by Potentiometric method or Wheatstone bridge respectively. However the biggest challenge nonetheless lies in signal to noise ratios.

Jedema et al [22] have shown an effective method to measure spin accumulation and relaxation in an all metal mesoscopic valve at even room temperature. They used a 4 terminal geometry to inject current between two terminals and measure voltage between the other two terminal. In this way, a voltage measuring path was isolated from the current flow and hence effects such as anomalous magnetoresistance, hall effect and spin dependent interface scattering did not affect the signal measured. (fig. 19). This geometry further shows clearly that ΔR for parallel and antiparallel alignment of Py electrodes will only be non zero if densities of spin injected at the cross of Cu electrodes are unequal (if a spin accumulation exists). The distance between Py electrodes was then varied to measure ΔR and hence quantify spin accumulation in copper. To measure such effects in semiconductors optical detection of spin injection has been successfully demonstrated by using circularly polarized light, however these still have not been done at room temperature. [22]

Among the dominant factors of precessional decoherence are due to spin orbit coupling, doping and crystal orientation. What is required therefore is a resistance of electron spin states to the environmental sources of decoherence. Optical pulses have been shown to be quite effective in achieving this. [23] These are used to create a superposition of spin states (the -

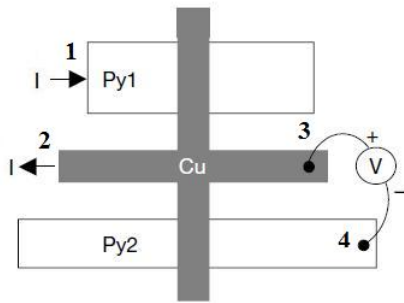


Figure 19. Schematic representation of the non-local measurement geometry to measure spin accumulation. Current is entering from contact 1 and extracted at contact 2. The voltage is measured between contact 3 and contact 4. [22]

basis defined by an applied magnetic field) that follow to the phase, amplitude and location of the resulting spin precession. The method works fine for bulk semiconductors, heterostructures and quantum dots. Later, the spatial selectivity and temporal resolution of optical techniques were used to monitor the decoherence and dephasing of electron spin polarization during transport through bulk semiconductors and across heterojunctions. [5] It was found that coherence is largely preserved as spins traverse across the junction over a broad range of temperatures. Fig. 20 shows this behavior and is clearly ballistic. Note that a phase shift at 0 is due to the difference in g factor of two materials and can be controlled by epitaxial growth techniques. [24]

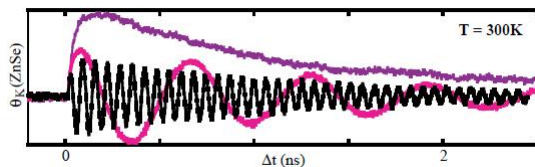


Figure 20. Room temperature transport across GaAs/ZnSe heterostructure. Coherent precessing spins injected into ZnSe measured through Kerr rotation at different magnetic field. $B=0$ (purple), $B=0.025\text{T}$ (Pink), $B=0.25\text{T}$ (black). [24]

Spin precession has also been electrically detected in diffusive metal. Jedema et al [25] first reported a controlled spin precession of electrically injected and detected electrons in a diffusive metallic conductor, using tunnel barriers in combination with metallic ferromagnetic electrodes as spin injector and detector. They first showed that the output of spin valve structure was sensitive to only spin degree of freedom. Therefore its sign could be changed by reversing the magnetization alignment. Thereafter, they further showed that diffusive spin precession could be controlled with perpendicular magnetic fields to observe a distinct angle rotation as big as 180 degrees where the sign of voltage reverses and reaches a maximum. (Figure 21)

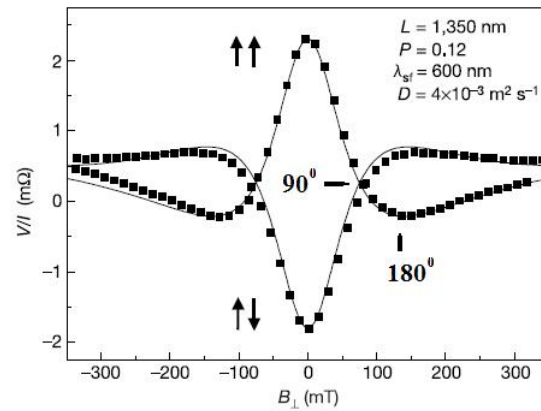


Figure 21. Diffusive spin precession measured through spin valve signal versus applied magnetic field. The signal shows an effective 90 degree ($v=0$) and 180 degree (voltage changes sign and maximum) precession. [25]

E. Spin torque

Also called spin transfer, Berger [26] showed that spin polarized current in a ferromagnet can exert a non-equilibrium exchange force on domain wall which in turn can be dragged along the direction of current. Of course an absence of external magnetic field is required with a further condition that the spin transfer force is large enough to overcome the coercivity of the free magnetic layer. This property opens up a gate for practical applications. firstly, the amount of spin current can be used to quantify the rotation of spins in free magnetic layer (a nanomagnet) and hence defining the bits for magnetic memory. Secondly, spin transfer can be used to setup a uniform spin wave in the nanomagnet which then can be used as the precessing spin filter to inject a coherent spin pulse in the semiconductor. Although the phenomenon shows a great potential for devices, the high amount of current needed to reorient the magnetization makes it commercially unfeasible. Another challenge is that in standard devices random thermal fluctuations may affect the precessional phase. However, absence of magnetic field in manipulation of the nanomagnets makes it a subject of extensive research of non volatile memory.

Stiles et al [27] used free-electron models and first principles electronic structure calculations (standard methods of quantum mechanics to compute transmission and reflection at an interface and then descriptions of spin currents for a distribution of electrons) to study the spin transfer torque. They attributed the origin of the angular momentum transfer to the absorption of transverse spin current by the interface. There are three distinct processes that contribute to the absorption

- 1) spin-dependent reflection and transmission
- 2) rotation of reflected and transmitted spins, and
- 3) spatial precession of spins in the ferromagnet.

When summed over all Fermi surface electrons, these processes reduce the transverse component of the transmitted and reflected spin currents to nearly zero for most systems of interest. Therefore, to a good approximation, the torque on

the magnetization is proportional to the transverse component of the incoming spin current. Quantitatively, they used the analogy between charge current and spin current to show that a spin current flowing in the x direction perpendicular to the interface delivers a torque per unit area,

$$N_C/A = (Q^{in} - Q^{tr} + Q^{ref}) \cdot \hat{x} \quad (26)$$

to a microscopically small region around the interface. Here Q^{in} , Q^{tr} and Q^{ref} are the incident, transmitted, and reflected spin currents computed using incident, transmitted, and reflected wave functions and when solved the one-electron stationary-state scattering problem. As explained further below, the transverse components of Q^{tr} and Q^{ref} are nearly zero due to spin filtering, differential spin reflection, and differential spin precession except for some cases. Consequently, the entire transverse spin current is absorbed and transferred to the magnetization in the immediate vicinity of the interface.

1) The spin-filter effect occurs because the wave function for an incident electron with a nonzero spin component transverse to the magnetization spin can always be written as a linear combination of spin-up and spin-down components. Then, because the reflection and transmission amplitudes differ for up and down spins, the up and down spin contents of the reflected and transmitted wave functions, which are spatially separated, differ both from each another and from the incident state. This effect manifests itself in spin current and as a result, the right side of eqn. 26 is nonzero.

2) The spin of an electron generally rotates when it is reflected or transmitted at the interface between a nonmagnet and a ferromagnet. The rotation is nonclassical and the amount of rotation differs considerably for electrons with wave vectors from different portions of the Fermi surface. Phase cancellation occurs when we sum over all electrons and hence transverse components of transmitted and reflected currents reduce to zero. However it is also found that phase cancellation for transmitted waves is not strong.

3) Due to exchange splitting, the electrons that transmit into the ferromagnet possess spin-up and spin-down components with the same total energy E_F , but different kinetic energy and so different wave vectors. This implies that each electron spin precesses in space as it propagates away from the interface. However, like the spin-rotation angles, the spatial precession frequency varies considerably over the Fermi surface. Consequently, rapid dephasing of the transverse spin components of the individual electrons occurs as the conduction electron ensemble propagates into the ferromagnet. The net result is a precessing spin current that damps out exponentially within a few lattice constants of the interface.

Kiselev et al [28] have recently showed that in addition to transfer of torque, a spin polarized current can be used to achieve oscillatory magnetic modes which are not attainable with magnetic fields alone. They argued that a simple magnetic-multilayer structure acts like a nanoscale motor that converts energy from a d.c. electrical current into high-frequency magnetic rotations that might be applied in new devices including microwave sources and resonators.

The device (all metallic mesoscopic spin valve) proposed by Jedema described in the last section can utilize the spin

precession and spin transfer torque to alter non-locally the magnetization of a ferromagnet electrode. The idea is to use a high density of spin polarized current in place of a large magnetic fields which have stray offshoots thus making the former more suitable. Further, by varying the length or time of flight, the precession angle can be controlled and so can the rotation of the magnetization. Though the device seems quite promising for a spin transistor its effectiveness is in doubt owing to high magnetic field required and small injection current. However, spin transfer torque can be better optimized with choice of materials.

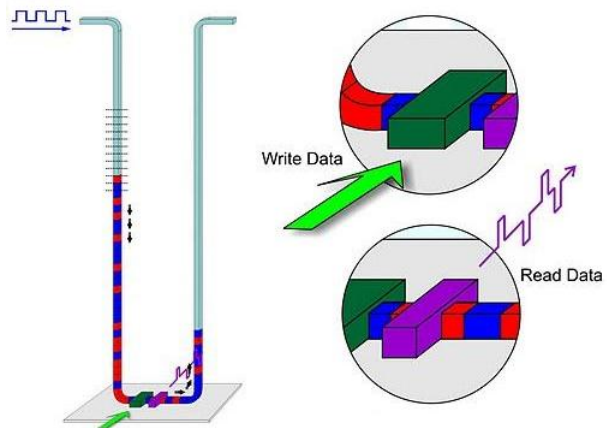


Figure 22. Vertical architecture of racetrack memory. Spin polarized currents transfer torques to push magnetic domains near read/write head to perform bit operations. [taken from internet]

One of the biggest impact of spin transfer torque has laid on production of fast and cheap memory. Led by Stuart Parkin IBM has been developing a "race track memory" suitable for MRAM and hard disks too. Racetrack memory uses spin coherent electric current pulses to move the magnetic domains along a nanoscopic permalloy wire. The domain patterns can be changed as they are made to move past a read/write heads located near them. [29] An architecture of this memory has been shown in figure 22. One of the limitations of this memory type is that the domains so far have been made to move only from microsecond pulses. A further research into it however shows a promise of making it up to nanosecond and hence 1000 times faster.

IV. FUTURE DEVICES AND CHALLENGES

A. Ferromagnetic semiconductor

Semiconductors form the heart of passive devices. Magnetic fields are required to capture and manipulate information carried by electronic spin. Future electronics hence demands that two properties are combined in one for further enhancement of their performance. With this we may also be able to inject spin polarized current into semiconductors which may allow quantum bit operations required for quantum computing. These have however not been realized for the following reasons. The magnetic g factors in conventional semiconductors are rather small and therefore there is no appreciable energy difference between the spin states. Also, the magnetic field required to

achieve this is quite high for practical uses. Although europium chalcogenides and semiconducting spinels have shown the potential to be magnetic semiconductor, their use is drastically limited due to notoriously difficult crystal growth. [30]

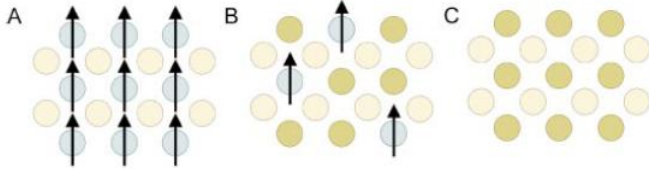


Figure 23. Three types of semiconductors: (A) a magnetic semiconductor, in which a periodic array of magnetic element is present; (B) a diluted magnetic semiconductor, an alloy between nonmagnetic semiconductor and magnetic element; and (C) a nonmagnetic semiconductor, which contains no magnetic ions. [30]

As previously explained a direct ohmic injection of spin polarized current is not efficient, though tunnel barriers have shown remarkable use there. Nonetheless, use of magnetic semiconductor instead of tunnel barrier could add another dimension to it. A direct approach to make semiconductor magnetic would be similar to making it a p-type or n-type through doping. This alloy of nonmagnetic semiconductors and magnetic elements is called diluted magnetic semiconductors (DMS). The kind of growth would then require that magnetic elements such as Mn could effectively replace cations from the parent system and also retain the ability to doping for creation of p-type or n-type extrinsic semiconductors. Molecular beam epitaxy (MBE) has allowed one to increase the solubility of such magnetic elements in semiconductors by forming single phase crystals at really low temperatures. Further, DMS needs to have a significant magnetic exchange interactions even at room temperature.

Ohno et al [31] displayed one such advantage of DMS. Using the property that GaAs/AlAs heterostructure is lattice matched, he showed spin dependent resonant tunneling through a double barrier tunnel diode AlAs/GaAs/AlAs with ferromagnetic p-type (Ga,Mn)As on one side and p-type GaAs on other side. The spin splitting of valence as well as conduction band occurs in the ferromagnetic semiconductor and hence using this difference in energy of splitting the structure shows filtering of holes of one spin type. It was further suggested that origin ferromagnetic exchange in this system is mainly due to RKKY interaction mediated by holes, however this has been not completely established.

B. Spin Hall effect

Hall effect has been a major discovery in the field of carrier transport in metals and semiconductors. First ordinary hall effect (OHE) and then were discovered quantum and fractional hall effects. Since electrons have spin in addition to charge, there arose speculations on the existence of spin hall effect. In ferromagnets, there are two contributions to the hall effect. One is due to external magnetic field (OHE) while the other

one arises because of the inherent magnetization of the system. The latter is called anomalous hall effect (AHE). The exact origin of this effect is not known however following reasoning has been well accepted. Spin imbalance in these systems have current polarized. Spin dependent resistivities have been defined in equation 1. The effects like scattering with phonon and impurities show themselves through spin orbit coupling and if the scattering in the material is spin dependent, up and down electrons scatter in opposite directions (see fig. 24) perpendicular to the electric field (generated through external voltage). The origin of this scattering can be understood in a classical way. The electrons like spinning tennis balls deviate in direction in air dependent on the manner of their rotation, the magnus effect. [29] The hall currents here hence will be asymmetrical producing hall voltage and spin accumulation and will be proportional to the inherent magnetization. [32] In other words, there exists spin accumulation in addition to charge accumulation at edges in AHE.

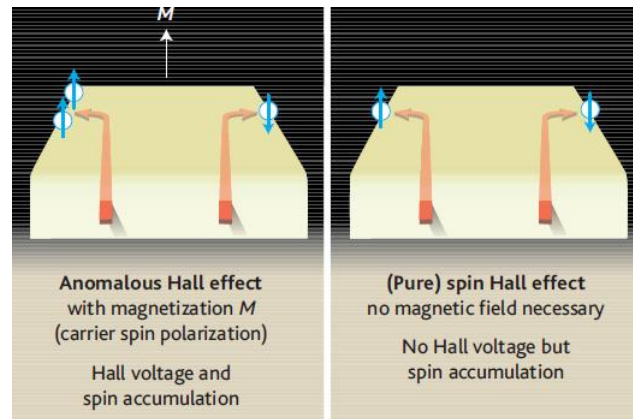


Figure 24. Spin hall effect in materials Left: anomalous hall effect Right: Pure Spin hall effect. [32]

If the spin orbit term is non vanishing and, even in the absence of magnetic field (a nonmagnet) spin dependent scattering can cause two spins to accumulate at the edges as shown in fig. 24 (right image). This is called pure spin hall effect. Although it does not really have hall voltage associated with it as two carriers in magnet are equal in number and effectively there builds no potential difference. The latter reason makes it hence quite difficult to study and establish the nature of SHE. However, there have been a couple of successful optical detection methods to measure spin accumulation at the edges of nonmagnetic semiconductors. [33] Above SHE is called extrinsic because of its dependence on asymmetry of the scattering. Another mechanism called intrinsic SHE has also been proposed. Here the deciding factor is the topological band structures of spin. Both mechanisms anyway arise out of the relativistic effect of electron motion or spin orbit interaction.

A noteworthy point here is that spin hall effects exist in nonmagnetic metals and hence can be used to effectively inject spins into other metals with compatible conductivities. This is then a conversion of normal charge current into spin polarized current. Saitoh et al [34] showed that spin current could be inversely transformed into charge current at room

temperature, termed inverse spin hall effect (ISHE). This phenomenon would be significant in spintronics processes such as the readout of quantum information in spin systems. In their sample system, a pure spin current J_S was injected from the $Ni_{81}Fe_{19}$ layer into the Pt layer using a spin pumping effect operated by ferromagnetic resonance FMR. See fig 25, here microwave was used to align the magnetization of the former layer in a fixed direction. Spin polarized current \vec{J}_s means that two electrons moving in opposite direction would have opposite spins. Owing to spin orbit coupling, these will bend in clockwise and anticlockwise directions with effective result that both accumulate in one direction as depicted in the figure 25. A charge current J_C is hence produced transverse to \vec{J}_s . If the spin polarization vector is given by σ (defined in equation 3), J_C can be related in a way similar to Lorentz electrodynamic force [34] where D_{ISHE} is a coefficient representing the ISHE efficiency.

$$J_C = D_{ISHE} J_S \times \sigma \quad (27)$$

By changing the spin-current polarization direction, the magnitude of this electromotive force was shown to vary critically, consistent with the prediction of ISHE. To check if the origin of this phenomenon was extrinsic or intrinsic SHE, similar measurements were performed with $Ni_{81}Fe_{19}/Cu$ and $Ni_{81}Fe_{19}/Nb$ systems which did not show any ISHE signal. It may support the intrinsic effect owing to the electronic structure of Pt, Cu and Nb. However the interface effect has to be studied to conclude its microscopic origin.

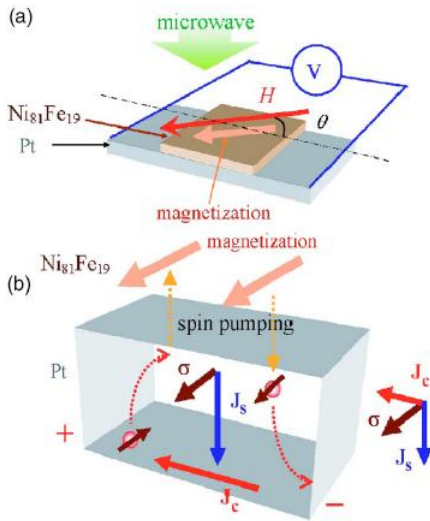


Figure 25. inverse spin hall effect a) the sample 8) Direction of spin polarized current J_S pumped and charge current J_C produced. [34]

An even more puzzling hall effect has recently shown by Wunderlich et al [35]. Similar to solar cells they designed GaAs p-n junction as shown in fig 26 a. The p-n junction has an associated built in voltage E which sweeps away the electron hole pair created in the depletion region by the incident light. And which in turns produces a voltage V_L along the direction of the charge current. Using circularly polarized

light however had an advantage to the solar cell. Spin orbit coupling of the electron spins together with photon's angular momentum cause them to align in a particular direction causing a spin polarized current. The holes lose the spin imbalance immediately in spite of strong coupling. Further, to due different scattering events hall voltage V_H develops in the material similar in magnitude to AHE. This is however not quite AHE since there was no external magnetic field nor was the material used magnetic (called spin injection hall effect).

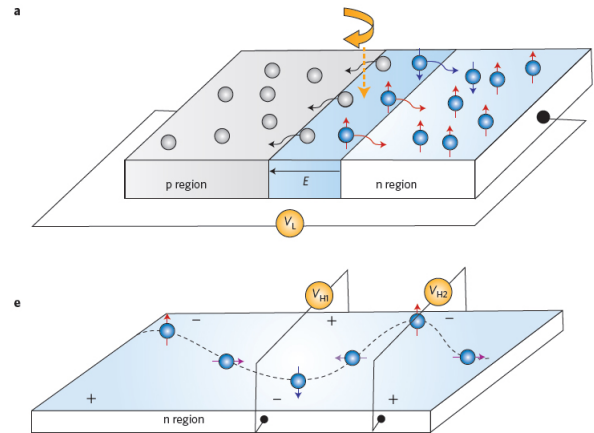


Figure 26. Injection spin hall effect (a) GaAs pn junction solar cell illuminated with circularly polarized light with built in voltage E and longitudinal voltage V_L (e) A spatial evolution of single electron in n region showing precession due to spin orbit coupling. [35]

A factor in generating a large V_H was the clever use of two-dimensional carrier confinement in a p-n junction and the choice of the growth direction of the planar structure to tailor the spin-orbit coupling and spin transport. It was shown that the degree of circularly polarized light was directly proportional to the transverse voltage signal and a polarization reversal reversed both the spin up/spin down imbalance and V_H . Shown in fig. 26 e, a net spin polarization of carriers is created away from the regions of measurement. A spatial evolution of a single spin shows an interplay of spin-dependent deflection and spin precession arising from an effective magnetic field due to spin-orbit coupling. The measured signal, an average over many electron spin trajectories, still preserves the depicted spatially changing transverse spin imbalance and V_H , which can even change sign. The measurements were performed at really low temperature. This is because at room temperature built in E vanishes and limits the practicality of the material. [35]

C. Graphene

The ease of processing, cost reductions and availability of resources have been major advantages of organic electronics. however, one property that tops other systems of materials in spintronics lies in the large spin lifetimes owing to small spin orbit coupling and hyperfine structure. This is because organic systems have light carbon atoms ($Z=6$), and spin orbit coupling that depends on Z^4 becomes rather small. Further, hyperfine interaction is very low since only 1% of

carbon (C^{13}) have nuclear moments. Graphene draws a further interest for its use in spintronics because of high mobility of carriers. Technically it can be considered as a semi metal or a semiconductor with zero band gap. Due to conical dispersion relations electrons and holes in graphene act like relativistic particles described by Dirac's equation with speed of light replaces by Fermi velocity of carriers ($\sim 10^6$ m/sec). According to experiments, the conductance of carriers through holes and electrons are the same reflecting identical mobilities for both. It has been also found that their mobilities hardly change between temperature 10k and 100k suggesting that dominant scattering mechanisms are due to defects. Owing to such high velocity and hence mobility, if the defect scattering could be eliminated graphene would have a resistivity much smaller than silver at room temperature. That together with its treacherous growth techniques has put a practical limitation so far. [29, 36]

Nikolaos et al [37] reported electronic spin transport and spin precession in single graphene layer using four terminal spin valve geometry. Importantly they observed that spin signal remained insensitive to the temperature variance. Further the spin relaxation length was found to vary between 1.5 and $2\mu\text{m}$ which is much larger than found for normal materials discussed in preceding sections. It was also hinted that their measurement was limited by extrinsic scattering which degraded amplitude of signals which could be improved by fabrication techniques. It is also believed that at low temperatures the reduction of the role of spin-orbit interaction by combining high-mobility graphene layers with quantum confinement would make it possible to increase the spin relaxation times considerably.

It was also realized later that graphene supports an extra quantum number called pseudospin because its honeycomb structure has two triangular sublattice. Wavefunction amplitudes then can be written like the two components of spin $1/2$ elementary particles (electrons) which in graphene show a relativistic fermionic nature. This also includes an effect called chirality the consequences of which are unusual sequencing of plateaus in measurement of quantum hall effect, suppression of back scattering at interfaces and Klein tunneling at interface. [38] In a monolayer of graphene, chirality means that the orientation of an electron's pseudospin is inextricably linked to the direction of its momentum. This then constrains the pseudospin to lie in the plane of the graphene sheet and thus limits its use as an independent tunable degree of freedom. In bilayers of graphene [39], the pseudospin degree of freedom is associated with the electronic density on the two layers. The constraint of chirality requires here that electronic density is equally divided between the two layers so that the pseudospin again lies in the plane of the layers but now turning twice as quickly as the direction of momentum. [39,40] However, if a voltage difference is created between layers, the asymmetry opens up a band gap. Further for states above or below the gap, an "up" or "down" component of pseudospin perpendicular to the electronic momentum and the plane of the sheet is created. [41] The electric field hence acts on the pseudospin in the same way as a magnetic field acts on the physical spin of electrons in spintronic applications. This preferred pseudospin

direction can be switched by inverting the sign of the applied potential difference.

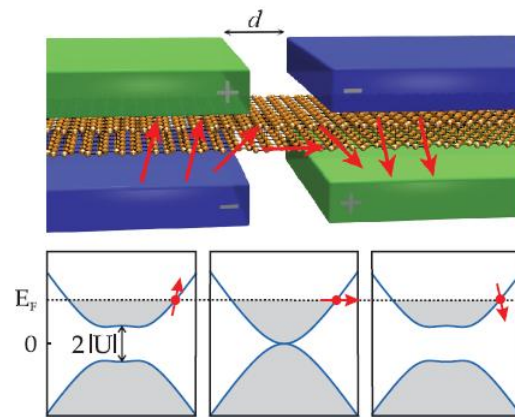


Figure 27. Top: Pseudospin-valve effect in bilayer graphene. Bottom: Schematic diagram of a pseudospin valve in bilayer graphene in its antiparallel (AP) configuration. [41]

Jose et al [41] have proposed a pseudospin valve exploiting the latter property of bilayer graphene and shown numerically that it should ideally have a large on-off ratios. The proposed structure is shown in figure 27. Top and bottom gates are used to independently control the Fermi level and the interlayer asymmetry, the latter hence creating an out-of-plane component of pseudospin. When the polarity of two gates is same, pseudospin components in side regions have same direction and electrons with energies above the gap flows with minimal resistance (parallel configuration). Conversely, when the device is in antiparallel configuration incoming pseudospins scatter at interface leading to high resistance and minimal current. This has been explained in following way. Similar to spin scattering at domain walls, the pseudospin of an incoming electron precesses about the changing local polarization as it tries to follow it. If the change in the polarization rotation is sharp enough (in antiparallel configuration), the realignment of the electron's pseudospin should be only partially successful, leading to reflection and a drop in the flow of current through the device.

Quite recently, use of graphene in spin filters has been proposed by Lundeberg [42] that uses quantum interference (weak localization). Although conductance fluctuations have been observed for several decades in a wide variety of materials, a direct measurement of their Zeeman splitting in graphene was first ever reported by them. Several factors were proposed to explain this. 1) Its low density of states enhances the visibility of conductance fluctuations and reduces the gate-voltage offset between spin split features 2) A small spin orbit coupling ensures two spin independent populations 3) Atomic scale flatness together with precise in plane magnetic field reduce effective Aharonov Bohm flux. This ability to distinguish conductance fluctuations associated with spin-up transport from those associated with spin-down transport, using the magnetic-field dependence of their position in gate voltage, may allow the development of interference-based spin filters in graphene.

D. Bychkov-Rashba structure asymmetry

Bychkov-Rashba spin splitting occurs in asymmetric quantum wells or in deformed bulk systems [43] and is an important phenomenon for spintronics. Such splitting induces a spin precession vector Ω in the Hamiltonian of the system.

$$\Omega(k) = 2\alpha_{BR}(k \times n) \quad (28)$$

where k denotes the wave vector for a Bloch state propagating in the plane with unit vector n and α_{BR} is a parameter depending on spin-orbit coupling and the asymmetry of the confining electrostatic potentials arising from the growth process of the heterostructure. This kind of splitting has also been found in nominally symmetric heterostructures with fluctuations in doping density. [21] The Bychkov-Rashba field quantified by Ω always lies in the plane, having a constant magnitude. The most appealing fact about structure inversion asymmetry is that α_{BR} can be tuned using simple application of electric field, providing an effective spin precession control without the need for magnetic fields. Another interesting feature of bulk and structure inversion asymmetry fields is that injection of electrons along a quasi-one-dimensional channel can lead to large relaxation times for spins oriented along $\Omega(k)$. [21]

Spin inversion asymmetry has inspired one of the earliest spintronic proposals by Datta and Das (described in following section) on a spin field-effect transistor in which α_{BR} is tailored by a gate. Consequently this has motivated a big research on spin inversion asymmetry. This tailoring, however, has not been completely understood. The microscopic origin of the Bychkov-Rashba Hamiltonian, and thus of the interpretation of experimental results on splitting in semiconductor heterostructures, has been often debated. The concerned Hamiltonian is generally understood to be arising from the electric field of the confining potential, (which may be present with an external bias), which acts on a moving electron in a transverse direction. The relativistic transformation then gives rise to a magnetic field through spin-orbit coupling acting on the electron spin. The parameter α_{BR} is then assumed to be directly proportional to the confining electric field. However this argument is generally misleading since the average electric force acting on a confined particle of uniform effective mass is zero. [21]

E. Spin transistors and qubits

1. *Spin Field Effect Transistor (SFET)*: First proposed by Datta and Das [44] the device is based on spin injection and spin detection by a ferromagnetic source and drain, and on spin precession about the built-in structure inversion asymmetry (Bychkov-Rashba) field Ω , in the asymmetric, quasi-one dimensional channel of an ordinary field-effect transistor. The attractive feature of the Datta-Das SFET is that spin-dependent device operation is controlled not by external magnetic fields, but by gate bias, which controls the spin precession rate. This has been shown in figure 28. The source (spin injector) and the drain (spin detector) are ferromagnetic metals or semiconductors, with parallel magnetic moments. The injected spin polarized electrons with wave vector k move ballistically along

a quasi-one-dimensional channel formed by, for example, an InGaAs/InAlAs heterojunction in a plane normal to n . The role of the gate is to generate an effective magnetic field (in the direction of Ω in Fig. 28, a 2D electron gas confined in plane with unit vector n has been considered), arising from the spin-orbit coupling in the substrate material, from the confinement geometry of the transport channel, and the electrostatic potential of the gate. This effective magnetic field causes the electron spins to precess. The magnitude of Ω is tunable by the gate voltage V_G at the top of the channel. The current is large if the electron spin at the drain points in the initial direction (top row) and small if the direction is reversed (bottom).

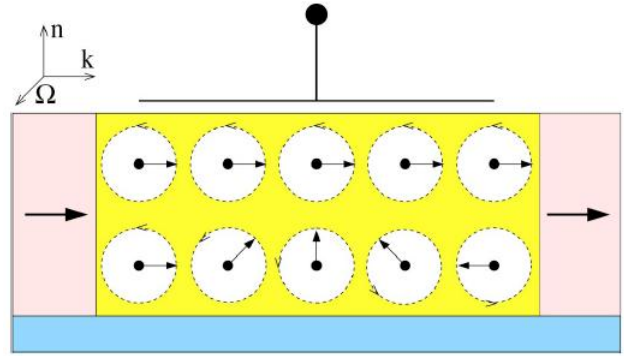


Figure 28. Datta-Das FET; at zero gate voltage, electron preserves spin state in transport channel Top: it enables current flow from source to drain. With applied gate voltage, electrons change their spin state from parallel to anti parallel to the direction of magnetization of ferromagnetic layer Bottom: this offers high resistance to flow of current. Therefore, electron scattering occurs at drain and no current flow from source to drain. [21]

Despite an unambiguous proposal, the device has not been realized so far for following reasons. a) The effective injection of spin polarized current from ferromagnet into 2DEG is quite problematic. b) Ballistic spin polarized transport needs to be realized through the channel with uniform Rashba coupling eliminating undesirable electric fields due to interface homogeneities. c) The Rashba spin orbit coupling should be controllable with gate voltage, this has been demonstrated though at low temperature [21] d) The structure inversion asymmetry should dominate over bulk inversion asymmetry and spin precession rate must be high enough for practical voltages to allow at least half precession.

2. *Magnetic Bipolar Transistor (MBT)*: The magnetic bipolar transistor (MBT) is a bipolar transistor with spin-split carrier bands and, in general, an injected spin source. Conceptually proposed this device can offer opportunities for effective spin injection, spin amplification or spin capacity i.e. changing non equilibrium spin density by manipulating voltage. This spin charge coupling can then have advantages in spin voltaic and giant magnetoresistance effects which are enhanced over the metallic systems by exponential dependence of current or biased voltage. [21] However this remains on paper unless ferromagnetic semiconductors are realized.

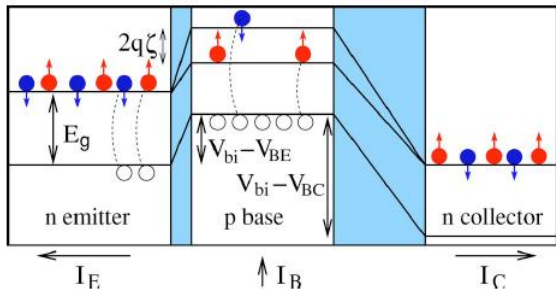


Figure 29. Scheme of an n-p-n magnetic bipolar transistor with magnetic base B, nonmagnetic emitter E and collector C operating in forward bias. [21]

Shown in figure 29 is an MBT with magnetic base B, non-magnetic emitter E and collector C. Non equilibrium spins in emitter are created via a spin injector (a ferromagnetic metal) attached to it. Another ferromagnet is attached at collector to modulate the current flow and control the amplification through current and magnetic field. Conduction and valence bands are separated by the energy gap E_g . The conduction band has a spin splitting $2q\zeta$, leading to equilibrium spin polarization P in the base. Depletion regions are represented by shaded regions. In the so-called forward active regime, where the transistor can amplify currents, the E-B junction is forward biased (here with voltage $V_{BE} > 0$ lowering the built-in potential V_{bi}), while the B-E junction is reverse biased ($V_{BC} < 0$). The directions of the different current I_C , I_B , I_E flows are indicated. Electrons flow from E to B, where they either recombine with holes (dashed lines) or continue to be swept by the electric field in the B-E depletion layer towards C. Holes in the base form mostly the base current, I_B , flowing to the emitter. The current amplification I_C/I_B hence can be controlled by P in the base as well as by the non-equilibrium spin in E.

3. *Hot electron spin transistor*: Spin transistors that rely on transport of hot (non thermalized) carriers have the potential of serving several they could be used as a diagnostic tool to characterize spin- and energy dependent inter-facial properties, scattering processes, and electronic structure, relevant to spintronic devices. [21] On the other hand, hot-electron transistors are also of interest for their ability to sense magnetic fields, their possible memory applications, and their potential as a source of ballistic hot-electron spin injection. A typical device of this nature looks like figure 14 with metal emitter and metal base anode being ferromagnetic. Different coercive fields of emitter and base region ensure independent switching of magnetization in presence of magnetic field. Further, a tunnel junction allows exploration of hot electrons over several volts above Fermi level. Forward bias V_{BE} controls the emitter current I_E of spin-unpolarized electrons, which are injected into a base region as hot carriers. The scattering processes in the base depending on its magnetization alignment with respect to emitter, together with the reverse bias V_{BC} , influence how many of the injected electrons can overcome the B/C Schottky barrier and contribute to the collector current I_C .

Similar to GMR, a magnetocurrent can be defined here by the ratio of difference between collector currents of different spins and their sum. Van Dijken et al [45] showed that for GaAs collector the magnetocurrent showed a non-monotonic behavior of current with change in V_{BE} . They argued that in addition to direct conduction band minima there is also an indirect minima at higher energy. After an initial decrease of magnetocurrent with electron energy larger than the base/collector Schottky barrier there is an onset of hot-electron transport into indirect minima valleys. Further, transistors with nonmagnetic collector and emitter with periodic stacks of ferromagnetic and insulator layer in base (fig. 15 and 16) have also been realized.

4. *Spin qubits in semiconductor nanostructures*: The possibility of using two level nature of electron spin to create a solid state quantum computer has been proposed. The idea is to manipulate spin states of a single electron using external magnetic field or microwaves for single qubit operations and then use the quantum exchange coupling between two neighboring electrons to carry out two qubit operations.

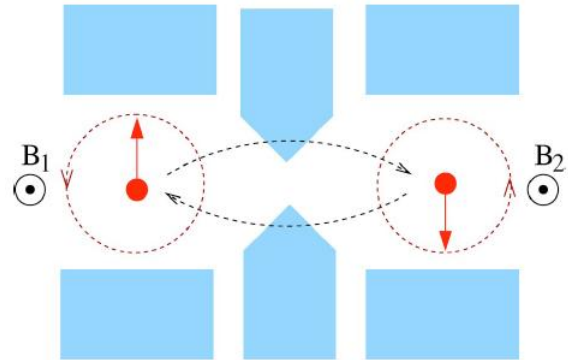


Figure 30. Architecture of a spin based quantum computing device. [21]

As shown in figure 30, Electrons are localized in electrostatically defined quantum dots, with coupling between electron spins via the exchange interaction allowed by tunneling between the dots. The tunneling can be controlled by gate voltage shown by shaded probes. Single-qubit operations are realized by single-spin precessions (circles dependent on direction of magnetic field), performed by applying local magnetic fields perpendicular to the plane to each dot. Two-qubit operations are indicated by the dashed arrow curves from left to right and vice versa. This proposal however assume that the predicted behavior will extend to many-spin systems, a requisite for practical quantum computation. This is far from being true. Experiments have not determined how spin-orbit and hyperfine interactions will affect the coherence of single electron spins as they are shuttled in tightly confined multiple quantum dot systems. Further, the control of spin dynamics and entanglement at the single-spin level in a semiconductor quantum dot structure is a nontrivial task, which has not been achieved even at mK temperatures despite experimental advances of this century. [21]

V. CONCLUSION

In conclusion we have seen how spin degree of freedom has provided us with myriad of opportunities in the field of electronics. While in one way it shows a great promise to increase power efficiency, cost reduction and size reduction are addition bonuses. Although much has been said on paper is actually not realized yet in practice. We have seen the devices in read heads and memory units based on spin electronics. However its boom in MRAM and spin transistors are far from its realization. The limits not only like in the proper lack of materials but also with complete understanding of the spin injection and transport science. Further, noise suppression poses a major challenge. The next batch of materials will probably resolve this issue. Also required are developments in fabrication and miniaturization of devices.

Spin relaxation and spin dephasing of conduction electrons is still not completely explored with only the basic principles well understood. What is needed are accurate band-structure derived calculations of spin relaxation times, in both metals and semiconductors. The same can be said of the g factor, calculation of which from first principles is a nontrivial task that has not been accomplished even for the elemental metals. [21] An important but quite controversial issue is spin relaxation and decoherence of localized or confined electrons where the hyperfine-interaction mechanism dominates. Furthermore, single-spin relaxation and decoherence, and their relation to the ensemble spin dephasing, need to be pursued further in the realization of quantum computing.

More specifically for spin electronics to flourish, we need materials that can sustain longer spin relaxation length and minimal scattering across materials and through interfaces. To integrate spins with passive charge electronics such as transistors, we are in a great need of ferromagnetic semiconductors or a technique to control spins in semiconductors. Again solubility and stability of magnetic ions in pure semiconductors are needed to facilitate a good exchange and undesired scattering of information. Further, spin injection in 2DEG has not been trivial and is still to conquer. With proper boundary conditions and material choice, one may hopefully integrate charge and spin circuits achieving amplification of one or both.

Among many problems, we have to understand some unconventional effects which we need to capitalize on. Spin hall effect together with materials choice and proper boundary conditions at the side contacts can help provide us with increased hall voltage and transverse spin accumulation. This then can be suitably injected across heterosystems. Further, Rashba spin splitting has a potential advantage of achieving effects similar to that created by a magnetic field using an applied electric field as proposed in Datta Das transistor. This will not only eliminate need of impractical amplitudes but also spurious effects of stray magnetic fields. Spin transfer torque is also one important aspect to pursue.

The spintronic devices have gone beyond GMR. Spin transfer torque has been used to induce a coherent microwave oscillations in nonmagnet [5]. Rudolph et al [21] have shown a spin laser which emits circularly polarized light upon recombination of unpolarized heavy holes with polarized elec-

trons. Further, a quantum computer has been conceptualized exploiting two level nature of the spin of electrons. With all this we can clearly say that spintronics is bound to shape the future of modern electronics that integrates two degrees of freedom of electrons in bringing about devices that are less dissipative, smaller in dimensions and have better reliability and performance.

REFERENCES

- [1] M. Baibich, A. Fert et al., Phys. Rev. Lett. 61, 2472 (1988).
- [2] J. Barnas, A. Fuss, R. Camley, P. Grunberg, W. Zinn, Phys. Rev. B 42, 8110 (1990).
- [3] G. Prinz, Science 282, 1660 (1998).
- [4] B. Dieny et al, IBM research division, PRB 45, 806 (1992).
- [5] S. A. Wolf et al, Science 294, 1488 (2001).
- [6] Terunobu Miyazaki et al, Physica B 237-238 (1997).
- [7] J.S. Moodera et al, Phys. Rev. Lett. 74, 3273 (1995)
- [8] Robert Fayfield et al, 7803-5240-8199, IEEE (1999).
- [9] Katti et al, J. Appl. Phys., vol. 91, 7245-7250 (2002).
- [10] <http://www.nve-spintronics.com/mram-operation.php>
- [11] Jadema PhD thesis, <http://dissertations.ub.rug.nl>
- [12] Fert et al el, Phys. Rev. B, Vol. 64, 184420 (2001).
- [13] E. I. Rashba, Phys. Rev. B 62, R16267 (2000).
- [14] Nozaki et al, Phys. Rev. Lett. 96, 027208 (2006).
- [15] H. Bru'ckl, Phys. Rev. B, H. 58/8893 (1998).
- [16] R. Mattana et al, Phys. Rev. Lett. 90, 166601 (2003).
- [17] Ian Appelbaum, arXiv:0910.2606v1 (2009).
- [18] Rippard and Buhrman, Phys. Rev. Lett., 84, 971 (2000).
- [19] Banerjee et al, Phys. Rev. Lett. 94, 027204 (2005).
- [20] Jansen, Banerjee Applied Phys. Lett. 90, 192503 (2007).
- [21] I. Zutic, J. Fabian and S. Das Sarma, Reviews of Modern Physics 76, (2004).
- [22] F. J. Jedema et al, Nature 410, 345 (2001).
- [23] J. A. Gupta et al Phys. Rev. B 59, R10421 (1999).
- [24] J. M. Kikkawa et al., Physica E 9, 194 (2001).
- [25] Jadema et al, Nature 416, 713 (2002).
- [26] L. Berger, Phys. Rev. B 54, 9353 (1996).
- [27] M. D. Stiles, A. Zangwill Phys. Rev. B 66, 014407 (2002).
- [28] S. I. Kiselev et al, Nature 425, 380 (2003).
- [29] <http://en.wikipedia.org/>
- [30] H. Ohno, Science 281, 951 (1998).
- [31] H. Ohno, et al ibid. 68, 2664 (1992).
- [32] Junichiro Inoue and Hideo Ohno, Science 309, 2004 (2005).
- [33] Y. K. Kato et al Science 306, 1910 (2004).
- [34] Satoh et al, App. Phys. Lett. 88, 182509 (2006).
- [35] Wunderlich, J. et al. Nature Phys. 5, 675-681 (2009).
- [36] Nikolaos PhD thesis, <http://dissertations.ub.rug.nl>
- [37] Nikolaos et al, Nature 448, 571 (2007).
- [38] K. S. Novoselov et al., Nature (London) 438, 197 (2005).
- [39] K. S. Novoselov et al., Nature Phys. 2, 177 (2006).
- [40] E. McCann and V. I. Fal'ko, Phys. Rev. Lett. 96, 086805 (2006).
- [41] P. San-Jose et al, PRL 102, 247204 (2009).
- [42] Mark B. Lundeberg and Joshua A. Folk, Nature Physics 5, 894 (2009).
- [43] E. I. Rashba, Sov. Phys. Solid State 2, 1109 (1960).
- [44] S. Datta and B. Das, Appl. Phys. Lett. 56, 665 (1990).
- [45] Van Dijken et al, Phys. Rev. Lett. 90, 197203 (2003).

ACKNOWLEDGEMENT

I would like to thank Prof. Bart van wees for his constant guidance and useful discussions throughout this review. I also acknowledge valuable help from dr. Tamalika Banerjee.



University of Groningen
Zernike Institute
for Advanced Materials